J Infect Chemother
DOI 10.1007/s10156-011-0312-4

NOTE

Bactericidal activity of topical antiseptics and their gargles against *Bordetella pertussis*

Takahisa Suzuki · Hiroshi Kataoka · Takashi Ida · Kazunari Kamachi · Takeshi Mikuniya

Received: 4 February 2011 / Accepted: 14 September 2011

Abstract *Bordetella pertussis* is the etiological agent of whooping cough, a common cause of respiratory illness in both children and adults. In the present study, we investigated the bactericidal activity of four antiseptics—povidone–iodine (PVP-I), benzethonium chloride (BEC), chlorhexidine gluconate (CHG) and benzalkonium chloride (BAC)—against *B. pertussis* ATCC9797 and clinical isolates. Among the topical antiseptics, PVP-I, BEC, and BAC, PVP-I and BAC in particular, showed high bactericidal activity, whereas CHG had low activity. PVP-I gargle also showed high bactericidal activity, similar to topical PVP-I. However, BEC gargle had low bactericidal activity. Our results indicate that topical PVP-I and BAC, and PVP-I gargle would be useful as effective antiseptics against *B. pertussis*.

Keywords *Bordetella pertussis* · Antiseptics · Bactericidal activity · Povidone–iodine · Benzalkonium chloride

Pertussis is an acute respiratory infection caused by the gram-negative coccobacillus *Bordetella pertussis* [1]. This disease is highly communicable, with a second attack rate of up to 90% among unvaccinated household contacts. *B. pertussis* is transmitted from an infected person to susceptible persons, primarily through aerosol droplets of respiratory secretions and secondarily through direct contact with the respiratory secretions. In Japan, the incidence of pertussis has been successfully decreased through the introduction of pertussis vaccines; however, there has been an increase in adult patients with pertussis since 2002 [2]. To prevent healthcare-associated bacterial pneumonia including pertussis, hand hygiene and disinfection of medical apparatus are strongly recommended for prevention of transmission of microorganisms [3]. In addition, oropharyngeal cleaning and decontamination with antiseptics are effective ways to prevent nosocomial respiratory infection [3, 4]. Although hand hygiene and oral rinse are recommended, no reports on the bactericidal activity of antiseptics against *B. pertussis* have been published. In the present study, therefore, the bactericidal activity of commercial topical antiseptics and their gargles against *B. pertussis* ATCC and clinical strains was determined.

Ten *B. pertussis* clinical isolates, collected from 2004 to 2008 in Japan, were investigated. The isolates were selected from the National Institute of Infectious Diseases (NIID) strain collections, according to their genotype (multilocus sequence type, MLST): five isolates, MLST-1; three isolates, MLST-2; one isolate, MLST-3; one isolate, MLST-4. The MLST-1 and MLST-2 strains were commonly isolated during the past two decades in Japan, but MLST-3 and -4 strains were not [2]. *B. pertussis* ATCC9797 was used as a laboratory strain. The *B. pertussis* clinical and ATCC9797 strains were cultured on Bordet–Gengou agar containing 15% defibrinated sheep blood for 48 h at 35°C, followed by subculture for 48 h. The following topical antiseptics and gargles were tested in

T. Suzuki · H. Kataoka · T. Ida · T. Mikuniya
Pharmaceutical Research Center, Meiji Seika Pharma Co., Ltd., Yokohama, Japan

T. Suzuki (✉)
Lifecycle Management Research Laboratory, Pharmaceutical Research Center, Meiji Seika Pharma Co., Ltd., Morooka-Cho 760, Kohoku-ku, Yokohama 222-8567, Japan
e-mail: takahisa.suzuki@meiji.com

K. Kamachi
Department of Bacteriology II, National Institute of Infectious Diseases, Tokyo, Japan

Published online: 04 October 2011

this study. The topical antiseptics were povidone–iodine (PVP-I; Isodine solution 10%; Meiji Seika Kaisha), benzethonium chloride (BEC; Hyamine solution 10%; Daiichi-Sankyo), chlorhexidine gluconate (CHG; Hibitane 20%; Dainippon Sumitomo Pharma), and benzalkonium chloride (BAC; Osvan S; Takeda Pharmaceutical). The gargle antiseptics were PVP-I (Isodine gargle solution 7%; Meiji Seika Kaisha) and BEC (Neostelin green 0.2% mouthwash solution; Nippon Shika Yakuhin).

Topical PVP-I, BEC, CHG, and BAC were diluted with sterile water at two or three concentrations according to the package insert instructions: PVP-I, 0.05–0.5%; BEC, 0.005–0.2%; CHG, 0.05–0.5%; BAC, 0.05% and 0.2%. The bacterial inoculum suspension and each antiseptic solution were mixed at 1:25 and incubated. After 0.25, 0.5, 1 and 3 min, 0.1 ml of the mixture was inoculated into 0.9 ml of neutralizer containing Tween 80, soybean lecithin, and sodium thiosulfate. Tenfold serial dilutions of each mixture were prepared, and 0.1 ml dilute solution was plated on Bordet–Gengou agar and incubated for 72 h at 35°C. The number of colonies was counted, and the number of colony-forming units (CFUs) in the mixture was calculated from the dilution rate [5].

Table 1 shows the bactericidal activity of the topical antiseptics against *B. pertussis* ATCC9797. A 0.25-min treatment with 0.05% PVP-I was found to successfully reduce the viable cells by more than 1×10^5 CFU/ml. A 0.25-min treatment with 0.05% BEC reduced the viable cells by more than 1×10^5 CFU/ml, whereas with 0.005% BEC, a 3-min treatment was required to achieve the same effect. A 0.25-min treatment with 0.05% BAC reduced the viable cells by more than 1×10^5 CFU/ml. With 0.05% or 0.2% CHG, even a 3-min treatment could not reduce the viable cells enough. To reduce the viable cells by more than 1×10^5 CFU/ml, treatment with 0.5% CHG for 3 min was required. This finding indicates that topical CHG has a lower bactericidal activity than topical PVP-I, BEC, and BAC against *B. pertussis* ATCC9797.

The bactericidal activity of topical PVP-I, BEC, and CHG against *B. pertussis* isolates was also investigated. The level of bactericidal activity is shown in Fig. 1. All isolates that received a 0.25-min treatment with 0.2% or 0.05% PVP-I had viable cells reduced by more than 1×10^5 CFU/ml. In contrast, with 0.005% BEC, a 3-min treatment was required to achieve the same effect. On the other hand, a sufficient decrease could not be achieved even when a 3-min treatment with 0.2% CHG was performed. With all the antiseptics, no marked differences were seen in terms of MLST and bactericidal effect. Table 2 shows the bactericidal activity of PVP-I and BEC gargles against *B. pertussis* ATCC9797. A 0.25-min treatment with 0.05% PVP-I gargle was found to reduce the viable cells by more than 1×10^5 CFU/ml, indicating that the PVP-I gargle had the same bactericidal activity as topical PVP-I. In contrast, with 0.2% BEC gargle, no significant decreases in viable cells were observed with 3-min treatment, although topical BEC has high bactericidal activity (Table 1).

To our knowledge, this is the first report on the bactericidal activity of antiseptics, especially PVP-I, against *B. pertussis*. Here, we show that topical PVP-I and BAC, and PVP-I gargle have high bactericidal activity compared with BEC and CHG. CHG is classified as a low-level antiseptic according to Spaulding's classification and shows variable bactericidal activity depending on the bacterial species. Furthermore, it was reported that a

Table 1 Bactericidal activity of topical povidone–iodine (PVP-I), benzethonium chloride (BEC), chlorhexidine gluconate (CHG), and benzalkonium chloride (BAC) against *Bordetella pertussis* ATCC9797

Antiseptic	Concentration (%)	Viable cells (CFU/ml)			
		0.25 min	0.5 min	1 min	3 min
PVP-I	0.5	–	–	–	–
	0.2	–	–	–	–
	0.05	–	–	–	–
BEC	0.2	–	–	–	–
	0.05	–	–	–	–
	0.005	8.5×10^6	1.3×10^6	3.0×10^3	–
CHG	0.5	1.8×10^7	1.1×10^7	1.4×10^6	–
	0.2	1.8×10^7	1.8×10^7	8.1×10^6	6.0×10^4
	0.05	3.0×10^7	2.5×10^7	1.9×10^7	1.9×10^6
BAC	0.2	–	–	–	–
	0.05	–	–	–	–

–, not detected ($<1 \times 10^2$ CFU/ml)

Initial cell concentration was $2.9–5.5 \times 10^7$ CFU/ml

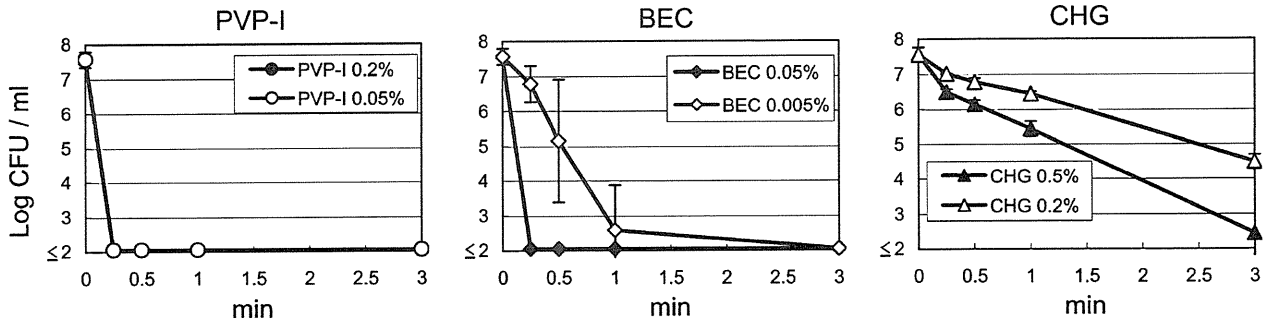

Fig. 1 Bactericidal activity of topical povidone–iodine (PVP-I), benzethonium chloride (BEC), and chlorhexidine gluconate (CHG) against *Bordetella pertussis* clinical isolates. Ten isolates [$\sim 5 \times 10^7$ colony-forming units (CFU)] were individually mixed with the topical antiseptic solution at different concentrations: PVP-I, 0.05% and 0.2%; BEC, 0.005% and 0.05%; CHG, 0.2% and 0.5%. After 0.25, 0.5, 1, and 3 min, the mixture was inoculated into a neutralizer. The number of viable cells was determined using plate count methods, and the number of CFUs in the mixture was calculated from the dilution rate. Detection limit was 1×10^2 CFU/ml

Table 2 Bactericidal activity of PVP-I and BEC gargles against *Bordetella pertussis* ATCC9797

Antiseptic	Concentration (%)	Viable cells (CFU/ml)			
		0.25 min	0.5 min	1 min	3 min
PVP-I	0.5	–	–	–	–
	0.2	–	–	–	–
	0.05	–	–	–	–
BEC	0.2	6.8×10^7	6.2×10^7	8.2×10^7	6.6×10^7
	0.05	8.5×10^7	8.9×10^7	7.5×10^7	4.4×10^7
	0.005	8.7×10^7	7.9×10^7	6.3×10^7	3.8×10^7

–, not detected ($<1 \times 10^2$ CFU/ml)

Initial cell concentration was $2.8–5.5 \times 10^7$ CFU/ml

relatively longer drug contact period is necessary for some bacterial species [6]. It is therefore not surprising that similar results were seen in this study with *B. pertussis*. It is not clear why the BEC gargle shows weak bactericidal activity. Similar findings were obtained in methicillin-resistant *Staphylococcus aureus* (MRSA) (data not shown); thus, the difference in bactericidal effect between topical BEC and BEC gargle is not considered to be an issue specific to *B. pertussis*. The BEC gargle contains several additive agents, e.g., polysorbate 80, mentha oil, spearmint oil, saccharin sodium, thymol, and sodium copper chlorophyllin. The additive agent(s) might be the cause of the low bactericidal activity against *B. pertussis*. Our findings indicate that equal effects of an active ingredient should not be expected when administered in different forms.

PVP-I is known to have potent broad-spectrum activity against bacteria, mycobacteria, fungi, and viruses [7], whereas BAC has no bactericidal activity against mycobacteria [8, 9]. Topical PVP-I and BAC have become widely used as antiseptic and disinfectant in hospitals, and PVP-I gargle is generally used for oral disinfection in Japan, especially at the time of year when the common cold and influenza are prevalent. *B. pertussis* frequently causes hospital and intrafamilial infections transmitted via aerosol droplets as well as the common cold and influenza. In light of this, gargling with PVP-I would be important among household members and hospital patients.

Adolescents and adults are assumed to be the primary reservoir of *B. pertussis* and play a crucial role in the transmission of the microbe to infants and unvaccinated children [10–12]. Macrolide antibiotics, such as erythromycin, are widely used for treatment of patients with pertussis and are currently recommended for prophylaxis in the United States as well. However, erythromycin resistance in *B. pertussis* has been reported in the United States, with an occurrence rate of <1% [13]. Fluoroquinolones are also widely used to treat respiratory tract infections in adults. These antibiotics have excellent in vitro activity against *B. pertussis*; however, several quinolone-resistant strains of *B. pertussis* were recently found in Japan [14]. Considering the mechanism of antiseptics, disinfection and gargling with PVP-I may be an effective way to eliminate *B. pertussis* regardless of drug resistance.

In conclusion, topical PVP-I and BAC, and PVP-I gargle, have high bactericidal activity against *B. pertussis*. To prevent the spread of pertussis infections, PVP-I and BAC would be useful as effective antiseptics against *B. pertussis*.

Acknowledgments The authors thank Dr. Yoshichika Arakawa, National Institute of Infectious Diseases, for his considerable support in conducting this study.

References

1. Mattoo S, Cherry JD. Molecular pathogenesis, epidemiology, and clinical manifestations of respiratory infections due to *Bordetella pertussis* and other *Bordetella* subspecies. Clin Microbiol Rev. 2005;18:326–82.
2. Han HJ, Kamachi K, Okada K, Toyoizumi-Ajisaka H, Sasaki Y, Arakawa Y. Antigenic variation in *Bordetella pertussis* isolates recovered from adults and children in Japan. Vaccine. 2008;26:1530–4.
3. Guidelines for preventing health-care-associated pneumonia, 2003. Recommendations of CDC and the Healthcare Infection Control Practices Advisory Committee. MMWR Morb Mortal Wkly Rep 2004;53(RR-3):1–36.
4. DeRiso AJ, Ladowski JS, Dillon TA, Justice JW, Peterson AC. Chlorhexidine gluconate 0.12% oral rinse reduces the incidence of total nosocomial respiratory infection and nonprophylactic systemic antibiotic use in patients undergoing heart surgery. Chest. 1996;109:1556–61.
5. Yoneyama A, Shimizu M, Tabata M, Yashiro J, Takata T, Hikida M. In vitro short-time killing activity of povidone–iodine (Isodine® Gargle) in the presence of oral organic matter. Dermatology. 2006;212:103–8.
6. Shimizu M, Okuzumi K, Yoneyama A, Kunisada T, Araake M, Ogawa H, et al. In vitro antiseptic susceptibility of clinical isolates from nosocomial infections. Dermatology. 2002;204:21–7.
7. Zamora JL. Chemical and microbiologic characteristics and toxicity of povidone–iodine solutions. Am J Surg. 1986;151:400–6.
8. Rikimaru T, Kondo M, Oizumi K. Efficacy of common antiseptics against mycobacteria. Int J Tuberc Lung Dis. 2000;4:570–6.
9. Widmer AF, Frei R. Decontamination, disinfection, and sterilization. In: Murray PR, Baron EJ, Pfaller MA, Tenover FC, Yolken R, editors. Manual of clinical microbiology. 7th ed. Washington, DC: American Society for Microbiology; 1999. p. 138–64.
10. Birkebaek NH, Kristiansen M, Seefeldt T, Degn J, Møller A, Heron I, et al. *Bordetella pertussis* and chronic cough in adults. Clin Infect Dis. 1999;29:1239–42.
11. Hewlett EL, Edwards KM. Pertussis–not just for kids. N Engl J Med. 2005;352:1215–22.
12. von König CH, Halperin S, Riffelmann M, Guiso N. Pertussis of adults and infants. Lancet Infect Dis. 2002;2:744–50.
13. Wilson KE, Cassiday PK, Popovic T, Sanden GN. *Bordetella pertussis* isolates with a heterogeneous phenotype for erythromycin resistance. J Clin Microbiol. 2002;40:2942–4.
14. Ohtsuka M, Kikuchi K, Shimizu K, Takahashi N, Ono Y, Sasaki T, et al. Emergence of quinolone-resistant *Bordetella pertussis* in Japan. Antimicrob Agents Chemother. 2009;53:3147–9.

MicroRNA Regulation of Glycoprotein B5R in Oncolytic Vaccinia Virus Reduces Viral Pathogenicity Without Impairing Its Antitumor Efficacy

Mina Hikichi[1], Minoru Kidokoro[2], Takeshi Haraguchi[3], Hideo Iba[3], Hisatoshi Shida[4], Hideaki Tahara[1,5] and Takafumi Nakamura[1,6]

[Q1] [1]*Core Facility for Therapeutic Vectors, Institute of Medical Science, Tokyo University, Tokyo, Japan;* [2]*Department of Virology III, National Institute of Infectious Diseases, Tokyo, Japan;* [3]*Division of Host-Parasite Interaction, Institute of Medical Science, Tokyo University, Tokyo, Japan;* [4]*Division of Molecular Virology, Institute for Genetic Medicine, Hokkaido University, Sapporo-shi, Japan;* [5]*Department of Surgery and Bioengineering Advanced Clinical Research Center, Institute of Medical Science, Tokyo University, Tokyo, Japan;* [6]*RNA and Biofunctions, Precursory Research for Embryonic Science and Technology (PRESTO), Japan Science and Technology Agency, Kawaguchi-shi, Japan*

Vaccinia virus, once widely used for smallpox vaccine, has recently been engineered and used as an oncolytic virus for cancer virotherapy. Their replication has been restricted to tumors by disrupting viral genes and complementing them with products that are found specifically in tumor cells. Here, we show that microRNA (miRNA) regulation also enables tumor-specific viral replication by altering the expression of a targeted viral gene. Since the deletion of viral glycoprotein B5R not only decreases viral pathogenicity but also impairs the oncolytic activity of vaccinia virus, we used miRNA-based gene regulation to suppress B5R expression through let-7a, a miRNA that is downregulated in many tumors. The expression of B5R and the replication of miRNA-regulated vaccinia virus (MRVV) with target sequences complementary to let-7a in the 3′-untranslated region (UTR) of the *B5R* gene depended on the endogenous expression level of let-7a in the infected cells. Intratumoral administration of MRVV in mice with human cancer xenografts that expressed low levels of let-7a resulted in tumor-specific viral replication and significant tumor regression without side effects, which were observed in the control virus. These results demonstrate that miRNA-based gene regulation is a potentially novel and versatile platform for engineering vaccinia viruses for cancer virotherapy.

Received 16 September 2010; accepted 7 February 2011; advance online publication 00 Month 2011. doi:10.1038/mt.2011.36

INTRODUCTION

Oncolytic viruses are promising therapeutic agents for cancer and are currently under preclinical and clinical investigation.[1] For example, vaccinia virus is a potential oncolytic virus because it has broad tropism in mammalian cells, a fast replication cycle, and no risk of integration into the host genome.[2] The replication cycle of vaccinia viruses only requires about 8 hours and results in cell lysis and release of progeny viruses. Furthermore, there is no risk of the viral genome integrating into the host genome because vaccinia viruses complete their entire life cycle in the cytoplasm, unlike most other DNA viruses. However, since viral toxicity is a potentially serious problem, the virus has been engineered to reduce its pathogenicity while retaining its oncolytic properties.[3,4]

The attenuated, replicating vaccinia virus strain LC16m8 is an attractive backbone for engineering a novel oncolytic agent because the strain has an extremely low neurovirulence profile.[5,6] In addition, LC16m8 has been safely administered to >100,000 infants and adults for smallpox vaccination and induced levels of immunity similar to those of the original Lister strain without serious side effects.[5,7,8] LC16m8 was isolated from LC16mO, which is a clone that was isolated from Lister strain through LC16, by repeated passages in primary rabbit kidney cells and selection for their temperature sensitivities.[5,6] As a result of attenuation, LC16m8 has a single nucleotide deletion in the open reading frame of the B5R gene.[9,10] B5R is a 42 kDa glycoprotein that is involved in virus [Q2] morphogenesis, trafficking, and dissemination.[11–19] Previously, the *B5R* gene was deleted from LC16m8 to develop a more genetically stable strain, LC16m8Δ.[20] In this study, we first compared the oncolytic potential of B5R-negative LC16m8Δ with B5R-positive LC16mO in mouse xenograft tumor model to determine the contribution of B5R to the pathogenicity and oncolytic potential of vaccinia virus.

Two strategies have been proposed to reduce the pathogenicity of vaccinia virus in normal cells and selectively target its oncolytic effects to tumor cells. In one strategy, insertional inactivation of vaccinia virus genes encoding thymidine kinase and/or epidermal growth factor-like vaccinia growth factor inhibits pathogenic viral replication in normal cells, while retaining its therapeutic replication in tumor cells that constitutively express thymidine kinase at high levels and have strong activation of the epidermal growth factor receptor pathway.[3,4] Thus, the success of this approach requires complementation of the disrupted viral genes by-products that are specifically found in tumor cells. Another strategy, transcriptional

Correspondence: *Takafumi Nakamura, Institute of Medical Science, Tokyo University, Minato-ku, Tokyo 108-8639, Japan. E-mail: taka@ims.u-tokyo.ac.jp*

targeting, uses tissue-specific promoters to restrict the replication of oncolytic viruses that have been developed from DNA viruses, such as adenovirus and herpes simplex virus, to malignant tissues.[21,22] However, this approach is not applicable to vaccinia viruses due to its cytoplasmic life cycle. As a result, an alternative strategy is needed to reduce the pathogenicity of vaccinia virus without impairing its oncolytic activity.

In this study, we used microRNA (miRNA)-based regulation of B5R to specifically target the oncolytic effects of vaccinia virus to tumor cells. Although this strategy has been applied to the development of oncolytic viruses from other DNA[23,24] and RNA[25,26] viruses, this is first application of the strategy to vaccinia virus. miRNAs are small noncoding RNAs (~22 nucleotides) that repress gene expression by binding to complementary sequences in the 3′-untranslated region (UTR) of messenger RNAs.[27,28] These post-transcriptional regulators play important roles in the control of tissue specification, tumorigenesis, and tumor progression. Since many miRNAs are differentially expressed in different tissues[29] and tumors,[30] they can be used to selectively promote viral replication in tumor cells expressing low levels of miRNA while inhibiting viral replication in normal cells that express higher levels of miRNA. An example of such a miRNA is let-7a, which belongs to the let-7 family of miRNAs that has lower expression in many kinds of cancer cells than in normal cells.[31–36] We successfully developed a miRNA-regulated vaccinia virus (MRVV) with let-7a miRNA complementary target sequences in the 3′UTR of *B5R*. This MRVV selectively replicates and induces oncolysis in tumor cells without toxicity in normal cells.

[Q3]

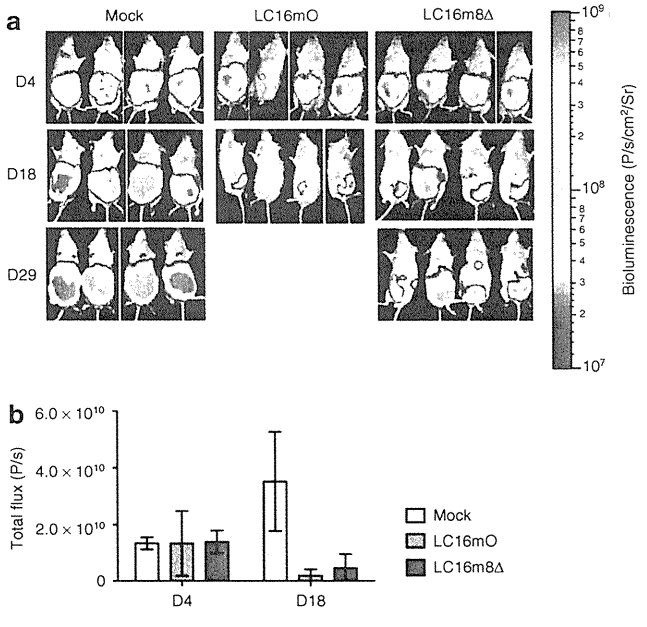

Figure 1 Comparison of the oncolytic effects of LC16m8Δ and LC16mO in mice bearing intraperitoneal xenografts. (**a**) BxPC-3 cells stably expressing luciferase (5 × 10^6 cells) were intraperitoneally injected into female severe combined immunodeficiency mice on day 0. Seven days after tumor implantation, the mice were intraperitoneally injected with a single dose of LC16mO or LC16m8Δ (1 × 10^7 plaque-forming unit/mouse). (**b**) *In vivo* tumor growth was monitored noninvasively by bioluminescence imaging after intraperitoneal administration of D-luciferin on days 4, 18, and 29. Quantification of the bioluminescence signals (photons/s) in the imaging data from days 4 and 18 in **a**. The data are presented as mean ± SD (n = 4).

RESULTS

Glycoprotein B5R is associated with viral pathogenicity and oncolytic activity

The *in vivo* oncolytic potentials of B5R-negative LC16m8Δ and B5R-positive LC16mO viruses in xenograft mouse model are compared in **Figure 1**. Four days after tumor implantation (day 4), the tumor growth in all of the implanted mice was similar. On day 18, tumor growth was significantly inhibited ($P < 0.001$) in both the LC16mO- and the LC16m8Δ-treated groups compared with the control group (**Figure 1a,b**). However, there was no significant difference in tumor volume reduction between the LC16mO- and LC16m8Δ-treated groups on this day (**Figure 1b**). In addition, all of the LC16mO-treated mice died or were sacrificed on days 21–28 because they exhibited symptoms of severe viral toxicity, such as weight loss and pock lesions on their tail, paws, face, and other areas of the body surface (data not shown). Although LC16m8Δ-treated mice did not show these symptoms, tumor regrowth was observed after day 29 (**Figure 1a**).

A schematic representation of the restoration of *B5R* in recombinant vaccinia virus LC16m8Δ-B5R is shown in **Figure 2a**. LC16m8Δ lysed A549, BxPC-3, Caco-2, and HeLa cells more efficiently than HEp-2, MDA-MB-231, PANC-1, and SK-N-AS cells. Although the cytolytic activity of LC16m8Δ was much lower than that of LC16mO in all tumors, B5R expression fully restored its oncolytic activity (**Figure 2b**).

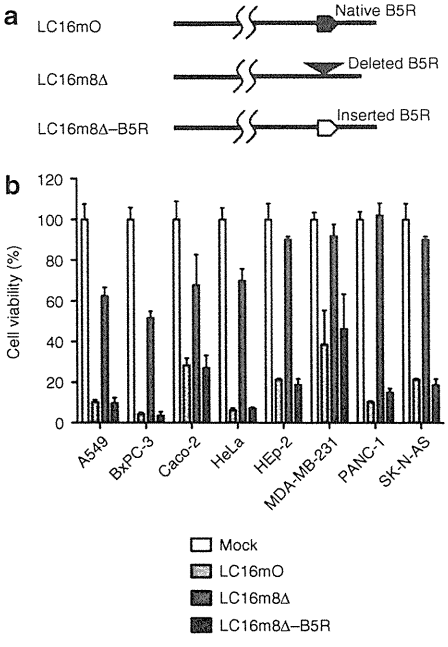

Figure 2 Relationship between B5R expression and oncolytic activity. (**a**) Schematic representation of the recombinant vaccinia virus LC16m8Δ-B5R. (**b**) Human cell lines were infected with B5R-positive or B5R-negative viruses at a multiplicity of infection of 0.5. The cell viabilities were determined 120 hours postinfection and are expressed as percentages of the cell survival of mock-infected cultures. The data are presented as mean + SD (n = 3).

B5R expression and the replication of miRNA-regulated vaccinia virus are dependent on endogenous let-7a

A schematic representation of MRVV with B5R-EGFP (BG) fusion protein (MRVV/BG) is shown in **Figure 3a**. The expression level of mature let-7a miRNA in normal human lung fibroblasts (NHLF) cells was three to four times higher than that in human lung and pancreatic carcinoma cell lines A549, BxPC-3, and PANC-1. On the other hand, there was less than a twofold difference in let-7a expression between NHLF and cervical carcinoma cell line HeLa (**Figure 3b**). These expression levels of let-7a correlate with functional activities of let-7a as measured by luciferase reporter assay. As shown in **Figure 3c**, the presence of four copies of let-7a target sequences in the 3′UTR of firefly luciferase (*FLuc*) mRNA in HeLa cells resulted in >96% of suppression of *FLuc* expression compared with the presence of four copies of the disrupted target sequences. In contrast, the suppression of *FLuc* expression in A549 and BxPC-3 cells was much weaker than that in HeLa cells. Thus, HeLa cells have five to seven times more let-7a activity than A549 and BxPC-3 cells (**Figure 3c**).

During infection of HeLa and NHLF cells, LC16m8Δ-B5Rgfp$_{let7a}$ did not induce a cytopathic effect (CPE) with B5R-enhanced green fluorescent protein (EGFP) expression, whereas LC16mO and the control viruses LC16m8Δ-B5Rgfp (lacking miRNA target sequences) and LC16m8Δ-B5Rgfp$_{let7a\text{-}mut}$ (containing the disrupted miRNA target sequences) resulted in a massive CPE after B5R-EGFP expression (**Figure 3d**). Simultaneously, the replication of LC16m8Δ-B5Rgfp$_{let7a}$ replication in HeLa and NHLF cells, which was equivalent to that of LC16m8Δ, was reduced by two log orders compared with that of LC16mO, LC16m8Δ-B5Rgfp, and LC16m8Δ-B5Rgfp$_{let7a\text{-}mut}$

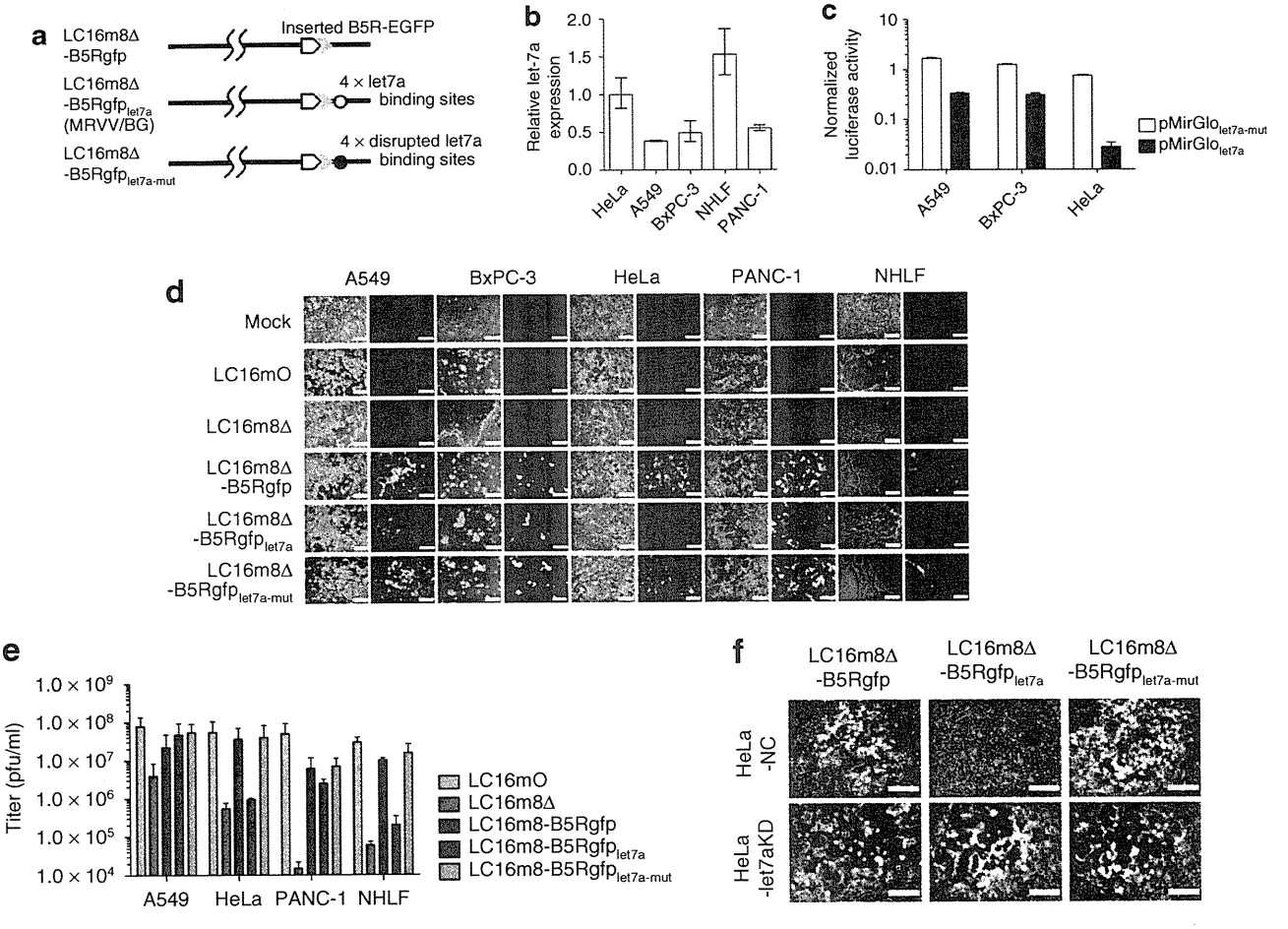

Figure 3 Construction and characterization of recombinant microRNA (miRNA)-regulated vaccinia virus (MRVV). (**a**) Schematic representation of the recombinant vaccinia virus genome showing the modified B5R protein fused with enhanced green fluorescent protein at its C-terminus (MRVV/BG). Four copies of let-7a miRNA complementary or disrupted target sequences, flanked by *NheI*/*AgeI* restriction sites, were incorporated into the 3′-untranslated region of the *B5R* gene. (**b**) Relative expression of mature let-7a miRNA in the indicated cell lines by real-time PCR analysis. The data are the let-7a level normalized with the U6 small nuclear RNA level relative to that in HeLa cells and are represented by the mean ± SD (n = 3). (**c**) The cell lines expressing different levels of let-7a were transfected with pMirGlo$_{let7a\text{-}mut}$ or pMirGlo$_{let7a}$ plasmid containing two expression units encoding firefly luciferase (*FLuc*) used as the primary reporter to monitor mRNA regulation and Renilla luciferase (*RLuc*) acting as a transfection control. Dual luciferase assay was performed 24 hours post-transfection. The *FLuc* activity is normalized to the *RLuc* activity. The data are presented as mean + SD (n = 3). (**d**) The cell lines expressing different levels of let-7a were infected with the MRVV/BG at an multiplicity of infection (MOI) of 0.1 and photographed using phase-contrast or fluorescence microscopy of the same field 3 days later. Bar = 200 μm. (**e**) One-step growth of the MRVV/BG was determined by titration of the viruses that were collected from the infected cells shown in **(d)**. The data are presented as mean + SD (n = 3). (**f**) HeLa-let7aKD cells (let-7a miRNA knockdown) or HeLa-NC cells (negative control) were infected with the MRVV/BG at an MOI of 0.1 and photographed 3 days later. The combined phase-contrast and fluorescence images are shown. Bar = 200 μm.

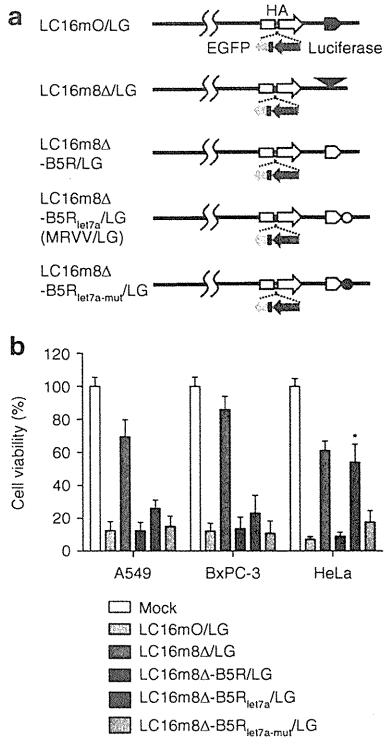

Figure 4 Effect of transgene insertion into microRNA (miRNA)-regulated vaccinia virus (MRVV) on its oncolytic activity *in vitro*. (**a**) Schematic representation of the recombinant vaccinia virus genome with the expression cassette that encodes both luciferase and enhanced green fluorescent protein reporters miRNA-regulated vaccinia virus (MRVV) luciferase (L) and enhanced green fluorescent protein (G) reporters (MRVV/LG). The symbols are the same as those used in **Figures 2a** and **3a**. (**b**) The cell viability after infection with MRVV/LG was determined as described in **Figure 2b**. The data are presented as mean + SD ($n = 3$). *$P < 0.001$ for LC16m8Δ-B5R$_{let7a}$/LG versus LC16m8Δ-B5R$_{let7a-mut}$/LG in HeLa cells.

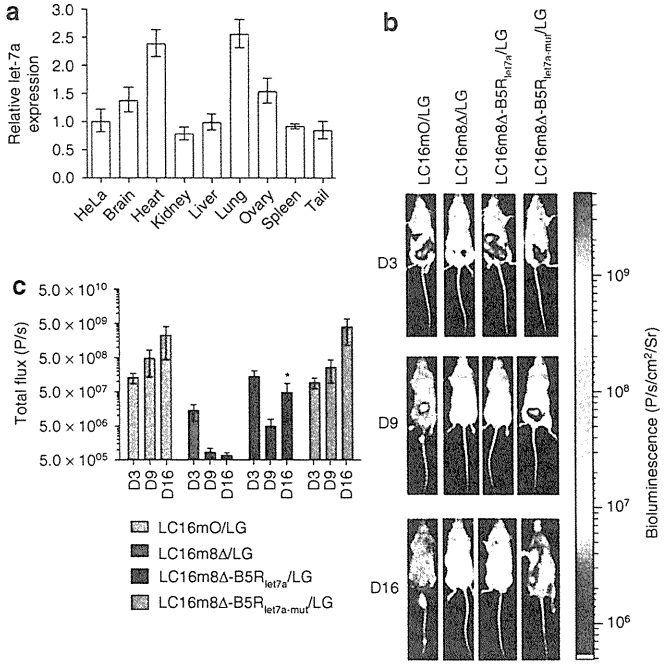

Figure 5 Biodistribution and replication of microRNA (miRNA)-regulated vaccinia virus (MRVV) luciferase (L) and enhanced green fluorescent protein (G) reporters (MRVV/LG) *in vivo*. (**a**) Relative expression of mature let-7a miRNA in the indicated mouse normal tissues by real-time PCR analysis. The data are the let-7a level normalized with the U6 small nuclear RNA level relative to that in HeLa cells and are represented by the mean ± SD ($n = 3$). (**b**) Representative images of the biodistribution of MRVV/LG in severe combined immunodeficiency mice that were intraperitoneally injected with 1×10^7 plaque-forming unit of MRVV/LG ($n = 3$). The biodistributions were visualized by intraperitoneal injection of D-luciferin at 3, 9, and 16 days after viral administration. The vaccinia virus designations are the same as those used in **Figure 4a**. (**c**) Quantitation of the bioluminescence signals in photons/s, calculated from the imaging data in **(b)**. The data are presented as mean ± SD ($n = 3$). *$P < 0.001$ for LC16m8Δ-B5R$_{let7a}$/LG versus LC16m8Δ-B5R$_{let7a-mut}$/LG on day 16.

(**Figure 3e**). In contrast, there were no differences in the CPE and replication in A549, BxPC-3, and PANC-1 cells among LC16m8Δ-B5Rgfp, LC16m8Δ-B5Rgfp$_{let7a}$, and LC16m8Δ-B5Rgfp$_{let7a-mut}$ (**Figure 3d,e**). Furthermore, the CPE and replication of LC16m8Δ-B5Rgfp, LC16m8Δ-B5Rgfp$_{let7a}$, and LC16m8Δ-B5Rgfp$_{let7a-mut}$ in A549, BxPC-3, and PANC-1 cells were comparable with those of LC16mO but were much greater than those of LC16m8Δ (**Figure 3d,e**). In addition, the presence of miRNA-based gene regulation was confirmed by using HeLa-let7aKD cells where TuD RNA largely suppresses endogenous let-7a activity (**Supplementary Figure S1**). LC16m8Δ-B5Rgfp$_{let7a}$ induced a CPE after B5R-EGFP expression in HeLa-let7aKD cells but not in HeLa-NC cells, although LC16m8Δ-B5Rgfp and LC16m8Δ-B5Rgfp$_{let7a-mut}$ showed a massive CPE after B5R-EGFP expression in both cell types (**Figure 3f**). Collectively, these results clearly demonstrate that B5R expression and the replication of LC16m8Δ-B5Rgfp$_{let7a}$ were regulated by endogenous let-7a.

Transgene insertion into microRNA-regulated vaccinia virus does not affect let-7a miRNA-regulated oncolytic activity

A schematic representation of MRVV with luciferase (L) and EGFP (G) reporters (MRVV/LG) is shown in **Figure 4a**. Although LC16m8Δ-B5R$_{let7a}$/LG lysed A549 and BxPC-3 cells with low levels of let-7a more efficiently than LC16m8Δ/LG, there was no significant difference in the oncolytic activities of LC16m8Δ-B5R$_{let7a}$/LG and LC16m8Δ/LG against HeLa cells with higher levels of let-7a (**Figure 4b**). In addition, the oncolytic activity of LC16m8Δ-B5R$_{let7a}$/LG was significantly lower than that of LC16m8Δ-B5R$_{let7a-mut}$/LG in HeLa cells; however, there was no significant difference in their oncolytic activities in A549 and BxPC-3 cells. Finally, LC16mO/LG, LC16m8Δ-B5R/LG, and LC16m8Δ-B5R$_{let7a-mut}$/LG showed a similar oncolytic effect against A549, BxPC-3, and HeLa cells. These results indicated that transgene insertion into the vaccinia virus genome did not affect let-7a miRNA-regulated oncolytic activity.

miRNA-based regulation of vaccinia virus inhibits viral replication in normal tissues

It has been reported that let-7a is highly conserved in humans and mice and is ubiquitous and abundant in normal tissues.[27,37,38] Similarly, we confirmed ubiquitous let-7a RNA accumulation in all mouse tissues tested (**Figure 5a**). Real-time PCR analysis showed that the brain, heart, lung, and ovary have higher expression level of let-7a than HeLa cells do, while the kidney, liver, spleen, and

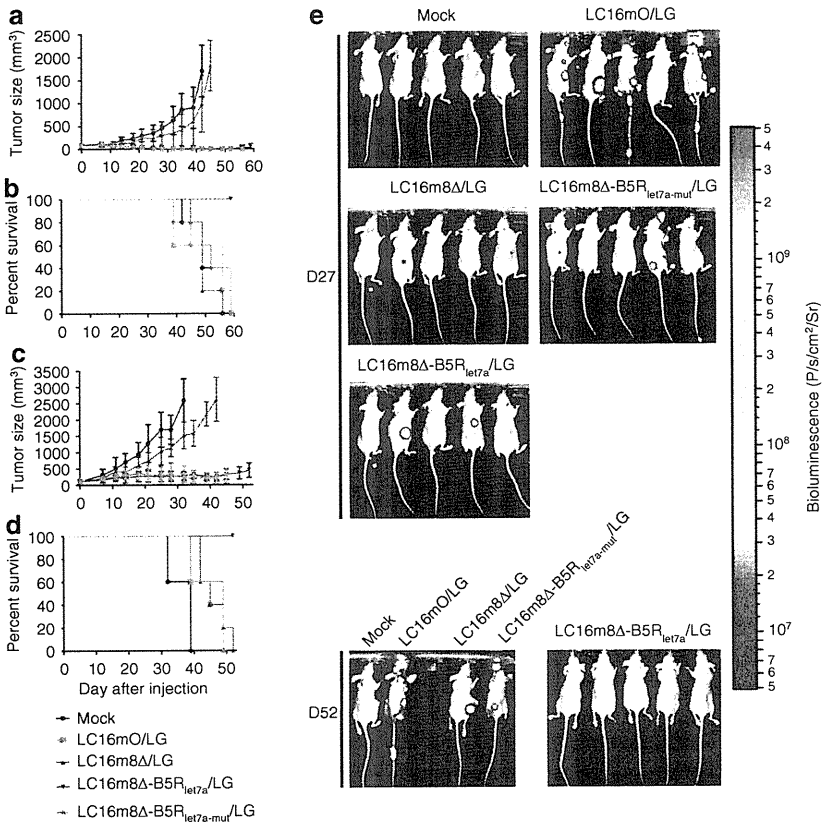

Figure 6 MicroRNA (miRNA)-regulated vaccinia virus (MRVV) luciferase (L) and enhanced green fluorescent protein (G) reporters (MRVV/LG) reduces viral pathogenicity while maintaining oncolytic activity *in vivo*. (**a**,**c**) Nude mice bearing established subcutaneous (**a**) BxPC-3 tumors or (**c**) A549 tumors were treated with intratumoral injections of MRVV/LG [1 × 10^7 plaque-forming unit (pfu)/injection, 3 × 10^7 pfu/mouse] on days 0, 3, and 6. The vaccinia virus designations are the same as those used in **Figure 4a**. The data are presented as mean ± SD (n = 5). (**b**,**d**) Survival curves of the mice that are shown in **a** and **c**. (**e**) *In vivo* biodistribution of MRVV/LG, determined by noninvasive imaging after intraperitoneal injection of D-luciferin into the mice that are shown in **(a, b)** on days 27 and 52.

tail have let-7a expression comparable to HeLa cells. Therefore, *in vivo* let-7a regulation was evaluated by a single intraperitoneal injection of each virus and noninvasive bioluminescence imaging in severe combined immunodeficiency (SCID) mice. Three days after injection of LC16mO/LG, LC16m8Δ/LG, LC16m8Δ-B5R$_{let7a}$/LG, or LC16m8Δ-B5R$_{let7a-mut}$/LG into SCID mice (day 3), the biodistribution of these viruses was concentrated in the abdomen. On days 9 and 16, the LC16mO/LG and LC16m8Δ-B5R$_{let7a-mut}$/LG viruses spread to several areas of their body, including the tail, paws, and face, where pock lesions were observed; however, the LC16m8Δ/LG and LC16m8Δ-B5R$_{let7a}$/LG viruses did not spread much (**Figure 5b**). In addition, there were significant differences in transgene expression levels and replication between LC16m8Δ-B5R$_{let7a}$/LG (or LC16m8Δ-/LG) and LC16m8Δ-B5R$_{let7a-mut}$/LG (or LC16mO/LG) on day 16 but not on days 3 and 9 (**Figure 5c**). To clear the relationship between B5R expression and the replication of MRVV in normal tissues, LC16m8Δ-B5Rgfp, LC16m8Δ-B5Rgfp$_{let7a}$, or LC16m8Δ-B5Rgfp$_{let7a-mut}$ was intraperitoneally injected into SCID mice, and the virus-associated B5R-EGFP expression was examined 15 days after injection. As expected, LC16m8Δ-B5Rgfp and LC16m8Δ-B5Rgfp$_{let7a-mut}$ caused pock lesions on the tail, where B5R-EGFP expression was detected. In contrast, no pock lesion and B5R-EGFP expression were observed on the tail of LC16m8Δ-B5Rgfp$_{let7a}$-injected mice (**Supplementary Figure S2**). Taken together, these results demonstrate that let-7a miRNA-based regulation inhibits vaccinia virus replication in normal cells by downregulating B5R in cells infected with MRVV.

miRNA-regulated vaccinia virus reduces viral pathogenicity while maintaining oncolytic activity after tumor-specific replication in mouse tumor models

LC16m8Δ-B5R$_{let7a}$/LG induced a significantly stronger antitumor effect than LC16m8Δ/LG in nude mice with subcutaneous BxPC-3 tumors (P < 0.001 on days 39–45; **Figure 6a**) or A549 tumors (P < 0.001 on days 25–42; **Figure 6c**) without the severe viral toxicity associated with LC16mO/LG and LC16m8Δ-B5R$_{let7a-mut}$/LG. Furthermore, in the BxPC-3 model, four out of five LC16m8Δ-B5R$_{let7a}$/LG-treated mice showed complete tumor regression without any symptoms of toxicity at the end of the experiment. Similarly, in the A549 model, the LC16m8Δ-B5R$_{let7a}$/LG-treated mice showed reduced tumor growth but not complete tumor regression. Although the degree of tumor regression in the LC16mO/LG- and LC16m8Δ-B5R$_{let7a-mut}$/LG-treated mice was similar to that of the LC16m8Δ-B5R$_{let7a}$/LG-treated mice in both tumor models, all of the mice treated with the former viruses died or were sacrificed on days 39–59 due to severe viral toxicity, such as pock lesions and weight loss. Finally, all of the mock- or

LC16m8Δ-treated mice were sacrificed by the end of the experiment due to their great tumor burden. Thus, infection with the LC16m8Δ-B5R$_{let7a}$/LG virus resulted in a significantly longer survival than infection with any of the other viruses in both mouse xenograft models ($P < 0.005$; **Figure 6b,d**).

These results were confirmed by bioluminescence imaging, which showed tumor-specific replication of LC16m8Δ-B5R$_{let7a}$/LG in BxPC-3 xenografts (**Figure 6e**) and A549 xenografts (**Supplementary Figure S3**). Three and 10 days after intratumoral injection of LC16mO/LG, LC16m8Δ/LG, LC16m8Δ-B5R$_{let7a}$/LG, or LC16m8Δ-B5R$_{let7a\text{-}mut}$/LG (days 3 and 10), the biodistribution of these viruses was concentrated in the tumor in nude mice bearing BxPC-3 (data not shown) or A549 xenografts (**Supplementary Figure S3**). On day 20, the LC16mO/LG and LC16m8Δ-B5R$_{let7a\text{-}mut}$/LG viruses spread to several areas of their body, including the tail, paws, and face, where pock lesions were observed; however, the LC16m8Δ/LG and LC16m8Δ-B5R$_{let7a}$/LG viruses did not spread (**Supplementary Figure S3**). On day 27, there was no viral replication in three of the tumor-free mice treated with LC16m8Δ-B5R$_{let7a}$/LG, whereas two of the mice with reduced tumor growth still showed tumor-specific viral replication (**Figure 6e**). On day 52, no viral replication was observed in normal tissues after the tumor had regressed completely in all five mice. In contrast, on day 27, viruses had already spread from tumor to normal tissues even in the tumor-free mice treated with LC16mO/LG and LC16m8Δ-B5R$_{let7a\text{-}mut}$/LG. By day 52, all of the surviving mice had widespread viruses in their tail, paws, ears, and face (**Figure 6e**). Finally, LC16m8Δ/LG replication was tumor-specific; however, it was much slower than that of the other viruses, which resulted in weaker oncolytic activity (**Figure 6e** and **Supplementary Figure S3**).

DISCUSSION

The viral glycoprotein B5R plays important roles in packaging intracellular matured virions with membranes derived from the trans-Golgi network or early endosomes to form intracellular enveloped virions.[12,16,17] Intracellular enveloped virions are transported along microtubules to the cell periphery[15,18] where they adhere to the cell surface as a cell-associated enveloped virions. B5R, along with the A36R and A33R proteins, is also involved in the Src kinase-dependent process of forming actin-containing microvilli and releasing cell-associated enveloped virions from the cell surface to form extracellular enveloped virions (EEVs).[13,14] Since EEVs are critical for cell-to-cell and long-range virus spreading, B5R dysfunction markedly reduces the formation of EEVs and results in small viral plaques *in vitro* and highly attenuated viruses *in vivo*.[10,11,17,19,20]

In addition, this study demonstrated that the deletion of B5R weakens its oncolytic activity, as shown by the reduced antitumor efficacy of B5R-negative LC16m8Δ in mouse xenograft tumor models (**Figures 1a** and **6a,c**). These results were confirmed by replication of LC16m8Δ *in vivo*, which was not only spatially restricted within the injected tumor but also slower replicating than B5R-positive viruses (**Figure 6e** and **Supplementary Figure S3**). The EEV is also surrounded by a host cell-derived envelope that contains several host complement control proteins and a few exposed viral proteins.[39–41] Among these proteins, B5R is the only target for EEV-neutralizing antibodies.[39] Nevertheless, high EEV-producing strains of vaccinia virus spread between tumors more efficiently than low EEV-producing strains, even in the presence of EEV-neutralizing antibodies, in a syngeneic mouse tumor model.[42] Collectively, these results suggest that strategies that regulate the expression of B5R, such as miRNA, are promising approaches for engineering safe and effective vaccinia viruses for cancer virotherapy.

Recently, tumor-targeting approaches using miRNA have been used to develop oncolytic viruses based on adenovirus,[23] coxsackievirus A21,[26] herpes simplex virus 1,[24] and vesicular stomatitis virus.[25] The tumor-specific replication of these engineered viruses has decreased their pathogenic effects in normal tissues. For example, the insertion of miRNA target sequences for muscle-specific miRNA into coxsackievirus A21 decreased myositis without compromising antitumor activity.[26] Similarly, insertion of miRNA target sequences for hepatocyte-specific miRNA into adenovirus reduced hepatotoxicity.[23] Since vaccinia virus exhibits broad host cell tropism, we used tumor-suppressed miRNA rather than tissue-specific miRNA to develop the MRVV. In addition, we selected let-7a miRNA because the let-7 family of miRNAs is highly conserved and abundantly expressed in many types of normal cells.[27,38] However, the expression of let-7a is downregulated in tumor cells isolated from patients with breast,[31] hepatocellular,[32] lung,[33,34] melanoma,[35] and pancreatic[36] carcinomas.

For example, let-7a is reportedly expressed in ~50% of tumor cell lines and tumor tissues from patients with lung or pancreatic cancer at <20% of the expression in normal cells and tissues adjacent to the tumors.[33,36] Similarly, the expression of let-7a in the human A549 lung, BxPC-3 pancreatic, and HeLa cervical carcinoma cell lines used in this study was reduced by ~25, 30, and 65% of the expression in NHLF, respectively (**Figure 3b**). Remarkably, the HeLa cells have five to seven times more let-7a activity than the A549 and BxPC-3 cells despite an approximately twofold difference of let-7a expression between these cells (**Figure 3c**). Considering that it has been proposed that target suppression depends on a threshold miRNA concentration,[43] the concentration of let-7a in HeLa cells may be sufficient to reach the threshold expression level necessary for strong suppression. On the other hand, perfectly complementary target sites for let-7a of MRVV may be subject to regulation by all the other members of the let-7 family that are expressed in HeLa cells as described previously.[43] Anyhow, B5R expression and the replication of MRVV/BG were almost completely inhibited by let-7a miRNA-based regulation in not only the NHLF but also HeLa cells (**Figure 3d–f**). Furthermore, B5R-EGFP expression and the replication of MRVV/BG were also abrogated on the mouse tail that has let-7a expression comparable to HeLa cells (**Figure 5a** and **Supplementary Figure S2**). Our findings are consistent with previous reports concerning let-7a miRNA-based regulation of vesicular stomatitis viral[25] and polioviral[37] replication in HeLa cells and mouse models. In contrast, the expression of let-7a in the A549, BxPC-3, and PANC-1 cells was low enough to induce efficient replication of MRVV/BG in these tumor cells and xenografts, although the residual let-7a activity slightly repressed the B5R expression of MRVV/BG *in vitro* (**Figure 3d**) and *in vivo* (**Supplementary Figure S4**).

In a rare example, Kelly *et al.* showed that oncolytic coxsackie virus A21 with inserted muscle-specific miRNA target sequences escaped from the cellular miRNA system by mutation of the target inserts.[26] We did not find any indication of escaped mutants from LC16m8Δ-B5R$_{let7a}$/LG, as shown in the bioluminescence images of the BxPC-3 model (**Figure 6e**). Furthermore, sequence analysis did not show any mutations in the target inserts of LC16m8Δ-B5R$_{let7a}$/LG or LC16m8Δ-B5Rgfp$_{let7a}$ during cell culture passages. As reported previously,[20] B5R$^+$ revertants spontaneously emerged from LC16m8 by frameshift mutation resulting from a single nucleotide insertion at site just upstream of the deletion site in the open reading frame of the *B5R* gene. Since the MRVV has four copies of miRNA complementary target sequences for let-7a in the 3′UTR (and not the open reading frame) of the *B5R* gene, it is unlikely that a slight mutation would result in a significantly different phenotype, even if a mutation in these target inserts occurred during viral replication.

On the other hand, the spread of LC16m8Δ-B5R$_{let7a}$/LG was much less than that of the unregulated LC16mO/LG or the control LC16m8Δ-B5R$_{let7a\text{-}mut}$/LG in SCID mice and therefore did not cause any pock lesions in normal mouse tissues where let-7a is abundant (**Figure 5a–c**). However, quantitation of the bioluminescence signal from the luciferase-expressing vaccinia revealed that the LC16m8Δ-B5R$_{let7a}$/LG signal was still higher by 1–2 log orders than the B5R-deleted LC16m8Δ/LG signal (**Figure 5c**). These results suggest that miRNA-mediated inhibition of B5R expression may be overcome by miRNA saturation, which has been observed by Kelly *et al.* previously.[44] The possibility is also supported by another data that no B5R-EGFP expression was observed in HeLa cells infected with LC16m8Δ-B5Rgfp$_{let7a}$ at an multiplicity of infection (MOI) of 0.1 (**Figure 3d**); however, 100-fold higher input multiplicities of LC16m8Δ-B5Rgfp$_{let7a}$ allowed B5R-EGFP expression in HeLa cells (data not shown). Thus, more attention should be paid to miRNA saturation rather than to mutation of miRNA target inserts in designing vaccinia viruses for future use. In this regard, incorporation of different miRNA target sequences of more than one miRNA species might be one strategy to address the question of miRNA saturation.

In conclusion, we developed a highly attenuated MRVV with let-7a miRNA complementary target sequences in the 3′UTR of the *B5R* gene. This MRVV could selectively replicate and induce oncolysis in tumor cells without affecting normal cells, depending on the miRNA expression level. More generally, this study shows that control of viral replication and oncolytic activity by miRNA-based gene regulation provides a potentially novel and versatile platform for engineering vaccinia viruses for cancer virotherapy.

MATERIALS AND METHODS

Plasmid construction. The construction of all plasmids used in this study is described in the **Supplementary Materials and Methods**.

Cell culture. Human carcinoma cell lines [lung A549 (Ham's F12K); pancreatic BxPC-3, PANC-1 and neuroblastoma SK-N-AS (RPMI-1640); colorectal Caco-2, epidermoid HEp-2 (E-MEM); cervical HeLa and breast MDA-MB-231 (D-MEM)] and rabbit kidney-derived RK13 cells (E-MEM) were obtained from the American Type Culture Collection [Q4] [Q5] (Manassas, VA) and grown in their respective mediums (Wako, Richmond, VA) with 10% fetal bovine serum (Hyclone, Waltham, MA) at 37 °C in a humidified atmosphere with 5% CO_2. NHLF cells was purchased from TaKaRa Biomedicals and cultured according to the manufacturer's protocol. [Q6] HeLa-let7aKD or HeLa-NC cells were generated by infecting HeLa cells with lentivirus expressing tough decoy (TuD) RNA against let-7a or a negative control, respectively, with the human 7SK RNA polymerase III promoter,[45] as described previously.[46] Single HeLa-let7aKD or HeLa-NC cell isolates were expanded and selected in media containing 5 μg/ml puromycin (Sigma, St Louis, MO). [Q7]

Virus construction. To construct viruses with B5R, namely, LC16m8Δ-B5R and LC16m8Δ-B5Rgfp, RK13 cells were infected with B5R-deleted LC16m8Δ viruses[20] at a MOI of 0.02, and then transfected with pB5R or pTN-B5Rgfp. After harvesting the progeny viruses 2–5 days later, LC16m8Δ-B5R and LC16m8Δ-B5Rgfp were selected on the basis of larger plaque size and/or enhanced EGFP expression, by three serial plaque purifications. Finally, the insertion of *B5R* was verified by sequencing the modified region.

Similarly, miRNA-regulated viruses, namely, LC16m8Δ-B5R$_{let7a}$, LC16m8Δ-B5R$_{let7a\text{-}mut}$, LC16m8Δ-B5Rgfp$_{let7a}$, and LC16m8Δ-B5Rgfp$_{let7a\text{-}mut}$ were constructed by infecting RK13 cells with LC16m8Δ viruses, as described above, and then transfecting them with pTN-B5R$_{let7a}$ × 4, pTN-B5R$_{let7a\text{-}mut}$ × 4, pTN-B5Rgfp$_{let7a}$ × 4, or pTN-B5Rgfp$_{let7a\text{-}mut}$ × 4, respectively.

Likewise, the viruses expressing luciferase and EGFP, namely, LC16mO/LG, LC16m8Δ/LG, LC16m8Δ-B5R/LG, LC16m8Δ-B5R$_{let7a}$/LG, and LC16m8Δ-B5R$_{let7a\text{-}mut}$/LG, were constructed by infecting RK13 cells with LC16mO, LC16m8Δ, LC16m8Δ-B5R, LC16m8Δ-B5R$_{let7a}$, or LC16m8Δ-B5R$_{let7a\text{-}mut}$ viruses, respectively, as described above, and then transfecting them with pSFJvnc110-LucIRESgfp. All viruses were propagated and titrated in RK13 cells and stored at −80 °C.

Quantification of let-7a miRNA. First, total RNA was isolated from A549, BxPC-3, HeLa, PANC-1, and NHLF cells and also normal brain, heart, kidney, liver, lung, ovary, spleen, and tail of 6-week-old female athymic nude mice (Charles River Laboratories, Yokohama, Japan) using the [Q8] mirVana microRNA isolation kit (Ambion, Carlsbad, CA). Then, expres- [Q9] sion of mature let-7a miRNA and the endogenous control were quantified by real-time PCR using the TaqMan microRNA assay kit (Applied Biosystems, Carlsbad, CA) for has-let-7a miRNA and U6 small nuclear [Q10] RNA (snRNA), respectively. The relative expression of let-7a was calculated by using the comparative threshold method (Applied Biosystems User Bulletin No. 2).

Luciferase reporter assay. Cells in 96-well optical-bottom white plates (Nunc, Rochester, NY) were transfected with 0.1 μg of pMirGlo$_{let7a}$ or [Q11] pMirGlo$_{let7a\text{-}mut}$ plasmid containing two expression units that encode Renilla luciferase (*RLuc*) acting as a transfection control and *FLuc* with four copies of let-7a target sequences or the disrupted sequences in the 3′UTR respectively, using Fugene HD (Roche, Basel, Switzerland). At 24 [Q12] hours after transfection, the cells were analyzed for luciferase activities using the Dual-Glo Luciferase Assay System (Promega, Madison, WI). [Q13]

Viral infection. Each cell line was infected with a vaccinia virus at an MOI of 0.1 or 0.5 plaque-forming unit (pfu)/cell, respectively, in Opti-MEM medium (Invitrogen, Carlsbad, CA) for 1 hour at 37 °C in 24-well or [Q14] 96-well plates. Seventy-two hours after infection, the cells in the 24-well plate were photographed under phase-contrast or fluorescence microscopy. Subsequently, the infected cells were harvested into 1 ml of growth medium and sonicated to release the replicated viruses for titration in RK13 cells. One hundred twenty hours after infection, the viability of the cells in the 96-well plate was determined by using the CellTiter 96 AQueous cell proliferation assay kit (Promega).

In vivo *experiments.* The protocols for the following animal experiments were approved by the Animal Experiment Committee of the Institute of Medical Science, University of Tokyo, Japan.

In the first *in vivo* experiment, BxPC-3 cells stably expressing luciferase (5×10^6 cells in 100 µl of phosphate-buffered saline, pH 7.4) were intraperitoneally injected into 6-week-old female SCID mice (Charles River Laboratories) on day 0. Seven days later, the mice were administered a single intraperitoneal injection of LC16mO or LC16m8Δ (1×10^7 pfu in 100 µl of Opti-MEM per mouse). Control animals (mock therapy) were injected with 100 µl of Opti-MEM without any virus. To monitor *in vivo* tumor growth noninvasively, 150 µl of D-luciferin (15 mg/ml) was administered to the treated mice on days 4, 18, and 29. The mice were anesthetized with isoflurane before imaging the tumors with the IVIS [Q15] 100 bioluminescence imaging system (Xenogen, Hopkinton, MA). The bioluminescence signals were quantified according to the manufacturer's protocol.

In the second *in vivo* experiment, 6-week-old female SCID mice were intraperitoneally injected with a single dose of each vaccinia virus expressing luciferase (1×10^7 pfu in 100 µl of Opti-MEM per mouse) on day 0. To monitor the *in vivo* viral growth, D-luciferin was injected into the mice on days 3, 9, or 16, and then they were examined by bioluminescence imaging, as described above.

In the third *in vivo* experiment, subcutaneous tumors were established by injecting A549 or BxPC-3 cells (5×10^6 cells in 100 µl of phosphate-buffered saline, pH 7.4) into the right flank of 6-week-old female athymic nude mice (Charles River Laboratories). When the tumors reached 5–8 mm in diameter, the mice received three intratumoral injections of each vaccinia virus (1×10^7 pfu in 100 µl of Opti-MEM per mouse) on days 0, 3, and 6. Control animals (mock therapy) were injected with 100 µl of Opti-MEM without any virus. The mice were euthanized at the end of the experiment or when any of the following occurred: tumor burden exceeded 2,500 mm^3, tumor ulceration occurred, or symptoms of severe viral toxicity, such as pock lesions on body surfaces and weight loss of >30%, manifested. The diameter of tumors was measured three times per week, and the volume of a tumor was calculated according to the formula: volume = 0.5 × length × $width^2$. The virus biodistribution was determined by injecting D-luciferin into the mice on day 27 or 52, followed by bioluminescence imaging, as described above.

Statistical analysis. The differences in cytolytic activity, *in vivo* viral replication, and tumor burden between treatment groups were analyzed for statistical significance by one-way or two-way ANOVA and the Bonferroni test when ANOVA showed overall significance. P values <0.05 were considered to be statistically significant. Survival curves were constructed using the Kaplan–Meier method. Survival times were statistically analyzed by using the log-rank test. Data were analyzed using GraphPad Prism Ver 5 (GraphPad Software).

SUPPLEMENTARY MATERIAL

Figure S1. Inhibitory effects of TuD RNA on endogenous let-7a activity.

Figure S2. B5R expression of miRNA-regulated vaccinia virus in normal tissues.

Figure S3. Representative images of the biodistribution of MRVV/LG, determined by noninvasive imaging after intraperitoneal injection of D-luciferin into the mice that are shown in (**Figure 6c,d**) on days 3, 10, and 20.

Figure S4. B5R expression of miRNA-regulated vaccinia virus in subcutaneous mouse xenografts that expressed low levels of let-7a.

Materials and Methods.

ACKNOWLEDGMENTS

This work was supported by the Precursory Research for Embryonic Science and Technology (PRESTO) program in RNA and Biofunctions from the Japan Science and Technology Agency and partly supported by a Grant-in-Aid for Young Scientists (A) from the Ministry of Education, Culture, Sports, Science and Technology of Japan (to T.N.).

REFERENCES

1. Parato, KA, Senger, D, Forsyth, PA and Bell, JC (2005). Recent progress in the battle between oncolytic viruses and tumours. *Nat Rev Cancer* **5**: 965–976.
2. Moss, B (2001). Poxviridae: The viruses and their replication. In: Knipe, DM, Howley, PM eds. *Fields Virology*. Lippincott: Philadelphia, PA, pp 2849–2883.
3. Park, BH, Hwang, T, Liu, TC, Sze, DY, Kim, JS, Kwon, HC *et al.* (2008). Use of a targeted oncolytic poxvirus, JX-594, in patients with refractory primary or metastatic liver cancer: a phase I trial. *Lancet Oncol* **9**: 533–542.
4. Zhang, Q, Yu, YA, Wang, E, Chen, N, Danner, RL, Munson, PJ *et al.* (2007). Eradication of solid human breast tumors in nude mice with an intravenously injected light-emitting oncolytic vaccinia virus. *Cancer Res* **67**: 10038–10046.
5. Hashizume, K, Yoshikawa, H, Morita, M and Suzuki, K (1985). Properties of attenuated mutant of vaccinia virus, LC16m8, derived from Lister strain. In: Quinnan GV, ed. *Vaccinia Virus as Vectors for Vaccine Antigens*. Elsevier Science: Amsterdam, pp 421–428.
6. Kenner, J, Cameron, F, Empig, C, Jobes, DV and Gurwith, M (2006). LC16m8: an attenuated smallpox vaccine. *Vaccine* **24**: 7009–7022.
7. Saito, T, Fujii, T, Kanatani, Y, Saijo, M, Morikawa, S, Yokote, H *et al.* (2009). Clinical and immunological response to attenuated tissue-cultured smallpox vaccine LC16m8. *JAMA* **301**: 1025–1033.
8. Yamaguchi, M, Kimura, M and Hirayama, M (1975). Report of the National Smallpox Vaccination Research Committee: Study of side effects, complications and their treatments. *Clin Virol* **3**: 269–278.
9. Morikawa, S, Sakiyama, T, Hasegawa, H, Saijo, M, Maeda, A, Kurane, I *et al.* (2005). An attenuated LC16m8 smallpox vaccine: analysis of full-genome sequence and induction of immune protection. *J Virol* **79**: 11873–11891.
10. Takahashi-Nishimaki, F, Funahashi, S, Miki, K, Hashizume, S and Sugimoto, M (1991). Regulation of plaque size and host range by a vaccinia virus gene related to complement system proteins. *Virology* **181**: 158–164.
11. Engelstad, M and Smith, GL (1993). The vaccinia virus 42-kDa envelope protein is required for the envelopment and egress of extracellular virus and for virus virulence. *Virology* **194**: 627–637.
12. Hollinshead, M, Rodger, G, Van Eijl, H, Law, M, Hollinshead, R, Vaux, DJ *et al.* (2001). Vaccinia virus utilizes microtubules for movement to the cell surface. *J Cell Biol* **154**: 389–402.
13. Katz, E, Ward, BM, Weisberg, AS and Moss, B (2003). Mutations in the vaccinia virus A33R and B5R envelope proteins that enhance release of extracellular virions and eliminate formation of actin-containing microvilli without preventing tyrosine phosphorylation of the A36R protein. *J Virol* **77**: 12266–12275.
14. Newsome, TP, Scaplehorn, N and Way, M (2004). SRC mediates a switch from microtubule- to actin-based motility of vaccinia virus. *Science* **306**: 124–129.
15. Rietdorf, J, Ploubidou, A, Reckmann, I, Holmström, A, Frischknecht, F, Zettl, M *et al.* (2001). Kinesin-dependent movement on microtubules precedes actin-based motility of vaccinia virus. *Nat Cell Biol* **3**: 992–1000.
16. Schmelz, M, Sodeik, B, Ericsson, M, Wolffe, EJ, Shida, H, Hiller, G *et al.* (1994). Assembly of vaccinia virus: the second wrapping cisterna is derived from the trans Golgi network. *J Virol* **68**: 130–147.
17. Smith, GL, Vanderplasschen, A and Law, M (2002). The formation and function of extracellular enveloped vaccinia virus. *J Gen Virol* **83**(Pt 12): 2915–2931.
18. Ward, BM and Moss, B (2001). Visualization of intracellular movement of vaccinia virus virions containing a green fluorescent protein-B5R membrane protein chimera. *J Virol* **75**: 4802–4813.
19. Wolffe, EJ, Isaacs, SN and Moss, B (1993). Deletion of the vaccinia virus B5R gene encoding a 42-kilodalton membrane glycoprotein inhibits extracellular virus envelope formation and dissemination. *J Virol* **67**: 4732–4741.
20. Kidokoro, M, Tashiro, M and Shida, H (2005). Genetically stable and fully effective smallpox vaccine strain constructed from highly attenuated vaccinia LC16m8. *Proc Natl Acad Sci USA* **102**: 4152–4157.
21. Kuruppu, D and Tanabe, KK (2005). Viral oncolysis by herpes simplex virus and other viruses. *Cancer Biol Ther* **4**: 524–531.
22. Mathis, JM, Stoff-Khalili, MA and Curiel, DT (2005). Oncolytic adenoviruses - selective retargeting to tumor cells. *Oncogene* **24**: 7775–7791.
23. Cawood, R, Chen, HH, Carroll, F, Bazan-Peregrino, M, van Rooijen, N and Seymour, LW (2009). Use of tissue-specific microRNA to control pathology of wild-type adenovirus without attenuation of its ability to kill cancer cells. *PLoS Pathog* **5**: e1000440.
24. Lee, CY, Rennie, PS and Jia, WW (2009). MicroRNA regulation of oncolytic herpes simplex virus-1 for selective killing of prostate cancer cells. *Clin Cancer Res* **15**: 5126–5135.
25. Edge, RE, Falls, TJ, Brown, CW, Lichty, BD, Atkins, H and Bell, JC (2008). A let-7 MicroRNA-sensitive vesicular stomatitis virus demonstrates tumor-specific replication. *Mol Ther* **16**: 1437–1443.
26. Kelly, EJ, Hadac, EM, Greiner, S and Russell, SJ (2008). Engineering microRNA responsiveness to decrease virus pathogenicity. *Nat Med* **14**: 1278–1283.
27. Lagos-Quintana, M, Rauhut, R, Lendeckel, W and Tuschl, T (2001). Identification of novel genes coding for small expressed RNAs. *Science* **294**: 853–858.
28. Zeng, Y, Yi, R and Cullen, BR (2003). MicroRNAs and small interfering RNAs can inhibit mRNA expression by similar mechanisms. *Proc Natl Acad Sci USA* **100**: 9779–9784.
29. Lagos-Quintana, M, Rauhut, R, Yalcin, A, Meyer, J, Lendeckel, W and Tuschl, T (2002). Identification of tissue-specific microRNAs from mouse. *Curr Biol* **12**: 735–739.
30. Chen, CZ (2005). MicroRNAs as oncogenes and tumor suppressors. *N Engl J Med* **353**: 1768–1771.
31. Sempere, LF, Christensen, M, Silahtaroglu, A, Bak, M, Heath, CV, Schwartz, G *et al.* (2007). Altered MicroRNA expression confined to specific epithelial cell subpopulations in breast cancer. *Cancer Res* **67**: 11612–11620.
32. Gramantieri, L, Ferracin, M, Fornari, F, Veronese, A, Sabbioni, S, Liu, CG *et al.* (2007). Cyclin G1 is a target of miR-122a, a microRNA frequently down-regulated in human hepatocellular carcinoma. *Cancer Res* **67**: 6092–6099.

33. Takamizawa, J, Konishi, H, Yanagisawa, K, Tomida, S, Osada, H, Endoh, H *et al.* (2004). Reduced expression of the let-7 microRNAs in human lung cancers in association with shortened postoperative survival. *Cancer Res* **64**: 3753–3756.
34. Johnson, SM, Grosshans, H, Shingara, J, Byrom, M, Jarvis, R, Cheng, A *et al.* (2005). RAS is regulated by the let-7 microRNA family. *Cell* **120**: 635–647.
35. Müller, DW and Bosserhoff, AK (2008). Integrin beta 3 expression is regulated by let-7a miRNA in malignant melanoma. *Oncogene* **27**: 6698–6706.
36. Torrisani, J, Bournet, B, du Rieu, MC, Bouisson, M, Souque, A, Escourrou, J *et al.* (2009). let-7 MicroRNA transfer in pancreatic cancer-derived cells inhibits *in vitro* cell proliferation but fails to alter tumor progression. *Hum Gene Ther* **20**: 831–844.
37. Barnes, D, Kunitomi, M, Vignuzzi, M, Saksela, K and Andino, R (2008). Harnessing endogenous miRNAs to control virus tissue tropism as a strategy for developing attenuated virus vaccines. *Cell Host Microbe* **4**: 239–248.
38. Pasquinelli, AE, Reinhart, BJ, Slack, F, Martindale, MQ, Kuroda, MI, Maller, B *et al.* (2000). Conservation of the sequence and temporal expression of let-7 heterochronic regulatory RNA. *Nature* **408**: 86–89.
39. Bell, E, Shamim, M, Whitbeck, JC, Sfyroera, G, Lambris, JD and Isaacs, SN (2004). Antibodies against the extracellular enveloped virus B5R protein are mainly responsible for the EEV neutralizing capacity of vaccinia immune globulin. *Virology* **325**: 425–431.
40. Pütz, MM, Midgley, CM, Law, M and Smith, GL (2006). Quantification of antibody responses against multiple antigens of the two infectious forms of Vaccinia virus provides a benchmark for smallpox vaccination. *Nat Med* **12**: 1310–1315.
41. Vanderplasschen, A, Mathew, E, Hollinshead, M, Sim, RB and Smith, GL (1998). Extracellular enveloped vaccinia virus is resistant to complement because of incorporation of host complement control proteins into its envelope. *Proc Natl Acad Sci USA* **95**: 7544–7549.
42. Kirn, DH, Wang, Y, Liang, W, Contag, CH and Thorne, SH (2008). Enhancing poxvirus oncolytic effects through increased spread and immune evasion. *Cancer Res* **68**: 2071–2075.
43. Brown, BD, Gentner, B, Cantore, A, Colleoni, S, Amendola, M, Zingale, A *et al.* (2007). Endogenous microRNA can be broadly exploited to regulate transgene expression according to tissue, lineage and differentiation state. *Nat Biotechnol* **25**: 1457–1467.
44. Kelly, EJ, Hadac, EM, Cullen, BR and Russell, SJ (2010). MicroRNA antagonism of the picornaviral life cycle: alternative mechanisms of interference. *PLoS Pathog* **6**: e1000820.
45. Czauderna, F, Santel, A, Hinz, M, Fechtner, M, Durieux, B, Fisch, G *et al.* (2003). Inducible shRNA expression for application in a prostate cancer mouse model. *Nucleic Acids Res* **31**: e127.
46. Haraguchi, T, Ozaki, Y and Iba, H (2009). Vectors expressing efficient RNA decoys achieve the long-term suppression of specific microRNA activity in mammalian cells. *Nucleic Acids Res* **37**: e43.

Journal of Clinical Microbiology

Characterization of Mumps Viruses Circulating in Mongolia: Identification of a Novel Cluster of Genotype H

Minoru Kidokoro, Rentsengiin Tuul, Katsuhiro Komase and Pagbajab Nymadawa

J. Clin. Microbiol. 2011, 49(5):1917. DOI: 10.1128/JCM.02387-10.
Published Ahead of Print 16 March 2011.

JOURNAL OF CLINICAL MICROBIOLOGY, May 2011, p. 1917–1925 Vol. 49, No. 5
0095-1137/11/$12.00 doi:10.1128/JCM.02387-10

Characterization of Mumps Viruses Circulating in Mongolia: Identification of a Novel Cluster of Genotype H▽

Minoru Kidokoro,[1]* Rentsengiin Tuul,[2] Katsuhiro Komase,[1] and Pagbajab Nymadawa[2]

Department of Virology III, National Institute of Infectious Diseases, Tokyo, Japan,[1] and National Influenza Center, National Center for Communicable Diseases, Ulaanbaatar, Mongolia[2]

Received 25 November 2010/Returned for modification 6 January 2011/Accepted 8 March 2011

Although mumps virus is still causing annual epidemics in Mongolia, very few epidemiological and virological data have been reported. We describe here the first phylogenetic analysis data on the mumps viruses circulated in Mongolia in 2009. We detected 21 mumps virus cDNAs and obtained a virus isolate from 32 throat swabs of mumps patients in Ulaanbaatar, the capital of Mongolia. The phylogenetic analyses based on the 316 nucleotides of the small hydrophobic gene show that these sequences form a single cluster, with the closest relatedness to the viruses belonging to genotype H. According to the recommendation of the World Health Organization, Mongolian mumps viruses could be classified into a novel genotype because the divergence between new sequences and genotype H reference viruses is >5% (6.3 to 8.2%). However, additional analyses based on the fusion gene, the hemagglutinin-neuraminidase gene, and the whole-genome indicate that the divergences between the Mongolian isolate and other genotype H strains never exceed the within-genotype divergences of other genotypes. These results suggest that Mongolia strains should be included in genotype H and that the current criteria for mumps virus genotyping should be revised. We propose here that the Mongolian viruses should be classified as a new subgenotype termed H3. Since previous epidemiological studies suggested that genotypes H may be associated with central nervous system diseases, we evaluated the neurovirulence of the Mongolian isolate in the neonatal rat system. However, the virus does not exhibit prominent neurovirulence in rats.

Mumps is a common and highly contagious viral disease characterized by fever and swelling of the salivary glands. Although mumps infections are benign and usually not fatal, they rarely cause more serious neurological complications, such as aseptic meningitis, encephalitis, and deafness.

The mumps virus (MuV) belongs to a member of the genus *Rubulavirus* of the family *Paramyxoviridae* (8). It has a single-stranded, negative-sense, nonsegmented RNA genome of 15,384 nucleotides (nt). The genome contains seven transcription units that encode open reading frames for the nucleocapsid (N), phospho (P), matrix (M), fusion (F), small hydrophobic (SH), hemagglutinin-neuraminidase (HN), and large (L) proteins. Two envelope glycoprotein genes, F and HN, are 1,617 and 1,749 nt in length and encode 538 and 582 amino acids, respectively (11, 39, 40). These proteins are located on the virion surface and play cooperatively essential roles in virus entry into the host cells by causing viral attachment to the cell surface receptor molecules and subsequent membrane fusion (33, 40). The HN protein, in addition, is the major target for the humoral immune response in MuV infection and bears several neutralizing epitopes (10, 17, 21). The SH gene, which contains 316 nt and encodes 57 amino acids, is nonessential for viral replication, and its function is unclear (9, 31). Since the SH gene is the most genetically divergent region among whole MuV genes (4, 32), its sequence data have been mainly used as the minimum amount of information for the phylogenetic analyses of MuVs (2, 15, 23). However, it may not necessarily reflect the antigenic properties of MuVs. Although it is generally believed that MuV is serologically monotypic, 13 genotypes (A to M) have been proposed thus far (2, 4, 12–14, 18, 22, 29, 35–38, 42, 43). Because of its high divergence, SH gene-based genotyping of the circulating virus is useful for tracing the viral transmission and investigating the chronological and geographical distribution of MuV strains. Several MuV genotypes exhibit a differential geographical distribution. For instance, genotypes A, C, D, E, and H are mainly observed in the Western Hemisphere (1, 2, 13, 34), whereas genotypes B, F, and I are solely detected in Asia (16, 28, 30, 42). Some studies have reported the potential associations between genotypes C, D, H, I, or J and neuropathogenicity (28, 35, 36, 38).

In Mongolia, since no mumps vaccine is available, mumps outbreaks occur repeatedly. However, very few data on molecular epidemiology have been reported. We describe here the results of phylogenetic analyses on MuVs circulating in Mongolia. The present study is the first report of the current epidemiological situation of MuVs in Mongolia.

MATERIALS AND METHODS

Viruses. Wild-type MuV 02-49 strain (genotype J) was obtained from Niigata Prefectural Institute of Public Health and Environmental Sciences (Niigata, Japan). Odate-3 strain (genotype I) was obtained from Akita Prefectural Institute of Public Health (Akita, Japan). Viruses were propagated and titrated in Vero cells.

Clinical samples. Throat swabs were collected on days 0 to 6 after onset (2.4 days on average) from 32 mumps patients hospitalized in the Airborne Infection Ward of the National Center for Communicable Diseases (NCCD), Ulaanbaatar, from May to July 2009 (Table 1). All cases were confirmed by enzyme immunoassay (EIA). Serum samples were collected from all patients except one. These specimens were stored at −70°C temporarily and then transported to the

* Corresponding author. Mailing address: National Institute of Infectious Diseases, 4-7-1 Gakuen, Musashimurayama, Tokyo 208-0011, Japan. Phone: 81-42-561-0771. Fax: 81-42-567-5631. E-mail: kidokoro@nih.go.jp.

▽ Published ahead of print on 16 March 2011.

TABLE 1. Clinical specimens described in this study

Case	Age (yr)	Gender[a]	Specimen[b]	ELISA		RT-PCR	Virus isolation	MuV strain	Accession no.
				IgM	IgG				
1	21	M	TS, Se	19.3	4.0	+	−	MuVs-MNG09-016	AB598760
2	27	F	TS, Se	8.6	3.9	+	−	MuVs-MNG09-017	AB598761
3	19	F	TS, Se	13.1	3.9	+	−	MuVs-MNG09-018	AB598762
4	1	M	TS, Se	28.5	3.9	−	−		
5	25	M	TS, Se	24.4	4.0	−	−		
6	14	F	TS, Se	19.6	3.9	+	−	MuVs-MNG09-021	AB598763
7	19	M	TS, Se	27.5	3.8	+	−	MuVs-MNG09-022	AB598764
8	10	F	TS, Se	27.7	3.8	+	−	MuVs-MNG09-023	AB598765
9	28	F	TS, Se	13.6	3.1	+	+	MuVi-MNG09-024	AB600843
10	15	M	TS, Se	26.1	4.0	+	−	MuVs-MNG09-025	AB598766
11	15	M	TS, Se	17.0	2.0	+	−	MuVs-MNG09-026	AB598767
12	6	M	TS, Se	23.2	3.5	+	−	MuVs-MNG09-027	AB598768
13	10	F	TS, Se	6.4	4.0	−	−		
14	17	F	TS, Se	16.2	3.6	−	−		
15	22	M	TS, Se	23.4	4.0	−	−		
16	15	M	TS, Se	26.5	3.3	+	−	MuVs-MNG09-244	AB598769
17	20	M	TS, Se	25.6	4.0	−	−		
18	17	M	TS, Se	3.0	3.3	−	−		
19	11	M	TS, Se	19.8	3.8	+	−	MuVs-MNG09-247	AB598770
20	31	M	TS, Se	21.0	3.8	+	−	MuVs-MNG09-248	AB598771
21	34	M	TS, Se	20.3	4.0	−	−		
22	16	F	TS, Se	8.2	3.3	+	−	MuVs-MNG09-250	AB598772
23	33	F	TS, Se	8.5	2.4	−	−		
24	35	M	TS, Se	7.0	3.8	+	−	MuVs-MNG09-252	AB598773
25	23	M	TS, Se	15.9	4.0	+	−	MuVs-MNG09-253	AB598774
26	5	M	TS, Se	0.4	1.3	−	−		
27	14	M	TS, Se	14.2	3.8	+	−	MuVs-MNG09-255	AB598775
28	15	F	TS, Se	8.0	3.5	+	−	MuVs-MNG09-256	AB598776
29	22	F	TS, Se	24.8	4.0	−	−		
30	13	M	TS, Se	23.3	3.5	+	−	MuVs-MNG09-258	AB598777
31	17	M	TS, Se	1.7	2.3	+	−	MuVs-MNG09-259	AB598778
32	16	M	TS	ND[c]	ND	+	−	MuVs-MNG09-260	AB598779

[a] F, female; M, male.
[b] TS, throat swab; Se, serum.
[c] ND, not done.

National Institute of Infectious Diseases (NIID), Tokyo, Japan, and were stored at −80°C until analyzed.

Measurement of mumps specific IgG and IgM. A commercially available capture IgM EIA kit and a commercially available indirect IgG EIA kit (Denka Seiken Co., Ltd., Niigata, Japan) were used to determine mumps specific IgM and IgG levels of mumps patient sera. Both assays were performed and interpreted according to the manufacturer's instructions. The IgM antibody titer was designated as an antibody index by calculating the ratio of the optical density (OD) of the sample to the OD of the weakly positive control serum provided with the kit. An antibody index exceeding 1.20 was determined as positive. IgG antibody titers were calculated from the sample absorbance and the reference standard curve generated from the reference sera provided with the kit. IgG antibody titers of ≥4.0 were defined as positive.

Virus isolation. Throat swabs soaked in Eagle minimum essential medium were centrifuged at 1,500 × *g* for 10 min, and the supernatant was supplemented with 3% fetal bovine serum, 200 μg of streptomycin/ml, and 200 U of penicillin/ml and then inoculated onto Vero cells. The cells were cultured at 37°C, observed for 14 days, and harvested when the cytopathic effects (CPE) became prominent. Two blind passages were performed on all CPE-negative tissue cultures.

RNA extraction and RT-PCR. Viral genomic RNA was extracted from 200 μl of throat swab samples for SH gene sequencing or the same volume of MuVi-MNG09-024 strain culture fluid for full-genome sequencing by using a QIAamp viral RNA minikit (Qiagen, Tokyo, Japan) according to the manufacturer's instruction manual. To amplify the SH gene region, one-step reverse transcription-PCR (RT-PCR) was performed with the primers SHfw (5′-TCAAGTAGT GTCGATGATCTC-3′) and HNrv (5′-CATAGGGCCTCCCGCGGCATTCAC TATGAC-3′) by using a One-Step RNA-PCR kit (AMV) (TaKaRa, Kyoto, Japan) according to the manufacturer's instructions. A second PCR primer set, SHfw and SHrv (5′-AGCCTTGATCATTGATCATCC-3′), was designed to amplify genome positions 6130 to 6803 to sequence a 632-nt region including the entire SH gene.

In order to determine the entire genome sequence of the Mongolian isolate, RT-PCR was performed on extracted viral RNA with random hexamers by using a Transcriptor high-fidelity cDNA synthesis kit (Roche Applied Science, Tokyo, Japan) and seven sets of genome specific primers spanning the entire MuV genome. The second-round nested PCR was repeated using another seven sets of primer pairs. The resulting RT-PCR products were gel purified by using a QIAquick gel extraction kit (Qiagen) and then subjected to sequence analyses.

Sequence analysis. Nucleotide sequences were determined by using a BigDye Terminator v3.1 cycle sequencing kit using a 3130xl Genetic Analyzer (Applied Biosystems, Tokyo, Japan).

Nucleotide alignments and phylogenetic analysis were performed by CLUSTALW (version 1.83) using neighbor-joining and Kimura two-parameter methods. The statistical significance of a particular tree topology was evaluated by bootstrap resampling of the sequences 1,000 times. To determine the genotype of the Mongolia mumps sequences, we used the criteria that Jin et al. proposed and that the World Health Organization (WHO) recommended on the basis of the reference strain sequences that they assigned (15, 41). Subgenotyping for registered genotype H sequences conformed to the previous reports (23, 38).

The GenBank accession numbers of the nucleotide sequences obtained in the present study are found in Table 1.

Neurovirulence test in neonatal rats. We carried out a neurovirulence test in neonatal rats as previously described (24). Briefly, a litter of Lewis neonatal rats (<24 h old) (Charles River Japan Co., Ltd., Japan) were inoculated intracerebrally with 100 PFU of each MuV strain. Each litter consisted of six to seven

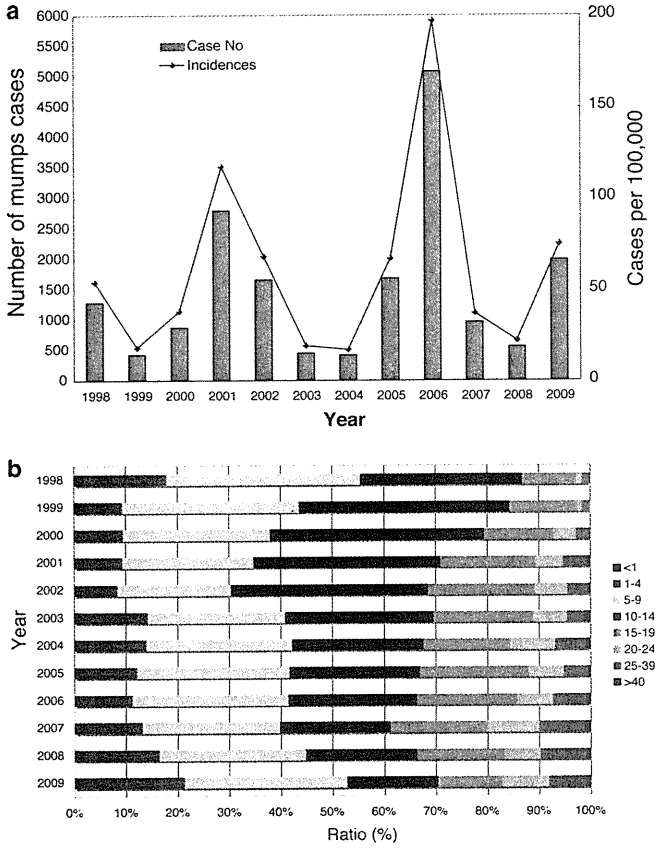

FIG. 1. Mumps activity in Mongolia from 1998 to 2009. (a) Annual reported mumps cases (bars) and incidence (solid line). (b) Component ratios (%) of age-specific incidence.

pups. We administered the MuV isolates MuVi-MNG09-024, 02-49, and Odate-3 in this test. After a month, magnetic resonance imaging was performed in the injected animals under anesthesia by using MRmini SA (DS Pharma Biomedical Co., Ltd., Osaka, Japan). On the basis of the scanned images, the neurovirulence test (NVT) score was calculated as the ratio of the cross-sectional area of the lateral ventricle to that of the entire brain in pixel units by using the image analysis software ImageJ (National Institutes of Health, Bethesda, MD). The differences in the scores were determined by using the Student t test, with $P < 0.05$ being the criterion for statistical significance.

RESULTS

Mumps epidemics in Mongolia. Since mumps vaccine is not available yet in Mongolia, mumps epidemics occur repeatedly with a periodicity of ~5 years (Fig. 1a). The most recent outbreak occurred in 2006 and was the largest in the past 11 years in Mongolia, i.e., 5,073 annual cases (an incidence of 197/100,000) were reported countrywide. The number of reported mumps cases in 2009, from the latest data, was 1,990 annual cases (an incidence of 75/100,000), which is an average outbreak, and most patients resided in Ulaanbaatar, the capital of Mongolia. According to age-specific incidence, the 5- to 14-year age group is the predominant group for all reported mumps cases (ca. 50 to 70%) (Fig. 1b). In contrast, the latest percentage of the 10- to 14-year age group had decreased to half of the ratio in 1998. In contrast, the >20-year age group has increased ~6 times over the past 11 years (Fig. 1b). However, the reasons for these phenomena are unclear.

Phylogenetic analysis of MuV sequences from clinical samples. We collected 32 throat swabs and 31 serum samples from 32 mumps patients (21 males and 11 females; age range, 1 to 35 years; mean age, 18 years 4 months) who were hospitalized in NCCD, Ulaanbaatar, from May to July 2009 (Table 1). Almost all serum samples (30 of 31 [96.7%]) were positive for IgM in an enzyme-linked immunosorbent assay, and their titers were very high (average, 16.9) (Table 1). In contrast, their IgG antibody titers were quite low (average, 3.5), and only nine samples (29.0%) were positive (Table 1). These results suggest that these mumps cases were primary infections.

We detected 21 MuV cDNAs and obtained one virus isolate (MuVi-MNG09-024) from the 32 mumps patient throat swabs (Table 1). No associations were found between epidemiological factors (age, gender, IgM antibody titer, and IgG antibody titer) and the MuV cDNA detection (data not shown). Although the detected sequences included seven different sequences (MuVi-MNG09-024, MuVs-MNG09-016, MuVs-MNG09-022, MuVs-MNG09-023, MuVs-MNG09-244, MuVs-MNG09-247, and MuVs-MNG09-248), as a result of phylogenetic analysis of the SH region (316 nt), these viruses were classified into an identical unique cluster (Fig. 2), and their divergence is within 2.2%. Among the all genotypes thus far identified, genotype H sequences exhibit the closest relatedness to Mongolian viruses. However, the genetic divergences between the new sequences and genotype H established reference virus sequences (Be1/UK88 and ManchS1/UK95) are more than 5% (6.3 to 8.2%). Since this result fulfills the proposed criteria for assigning a new MuV genotype (15, 41), it is plausible that Mongolian MuV sequences might be classified into a novel genotype. Meanwhile, the genotype H sequences of MuVs isolated in the late 1990s from Japan (SA475/JPN97) (37), Korea (Yeoju1498, Yeoju1502, Yeoju1503, and Yeoju1504) (19), and Switzerland (776273SHG and 776274SHG) (38), which were classified as members of subgenotype H2 (23, 38), are included in the same branch with our new sequences, and the divergences among some of these sequences are not necessarily >5% (4.1 to 6.3%) (Fig. 2). In addition, this cluster of viruses share the characteristic two conserved amino acid sequences at positions 19 and 26 (cysteine and isoleucine, respectively) in the SH gene (18) (Table 2). Therefore, in order to define more precisely the phylogenetic position of the Mongolian MuVs, we determined the whole-genome sequence of the isolated virus MuVi-MNG09-024, and additional analyses were performed on the sequences of the F gene (Fig. 3), HN gene (Fig. 4), and the whole genome (Fig. 5) of the isolate by comparison to the sequences available in the DDBJ/EMBL/GenBank databases. According to these results, the phylogenetic trees constructed from the F or HN or whole-genome sequences branch in the same manner mutually and compared to that based on the SH gene (Fig. 3 and 4). However, former divergences are much restricted compared to that of the SH gene. In particular, the divergences between the Mongolian sequences and other genotype H sequences are relatively low (0.5 to 1.6% in F genes, 1.3 to 3.1% in HN genes, and 2.0 to 2.3% in whole genomes) compared to that of the same set of the SH gene (5.4 to 7.9%). It should be noted that those divergences are equivalent to the within-genotype variability of other genotypes, (e.g., up to 4.9% in F, up to 4.9% in HN, and up to 2.7% in whole genomes). In addition, a high bootstrap value (e.g., >95%) is also another important index to confirm

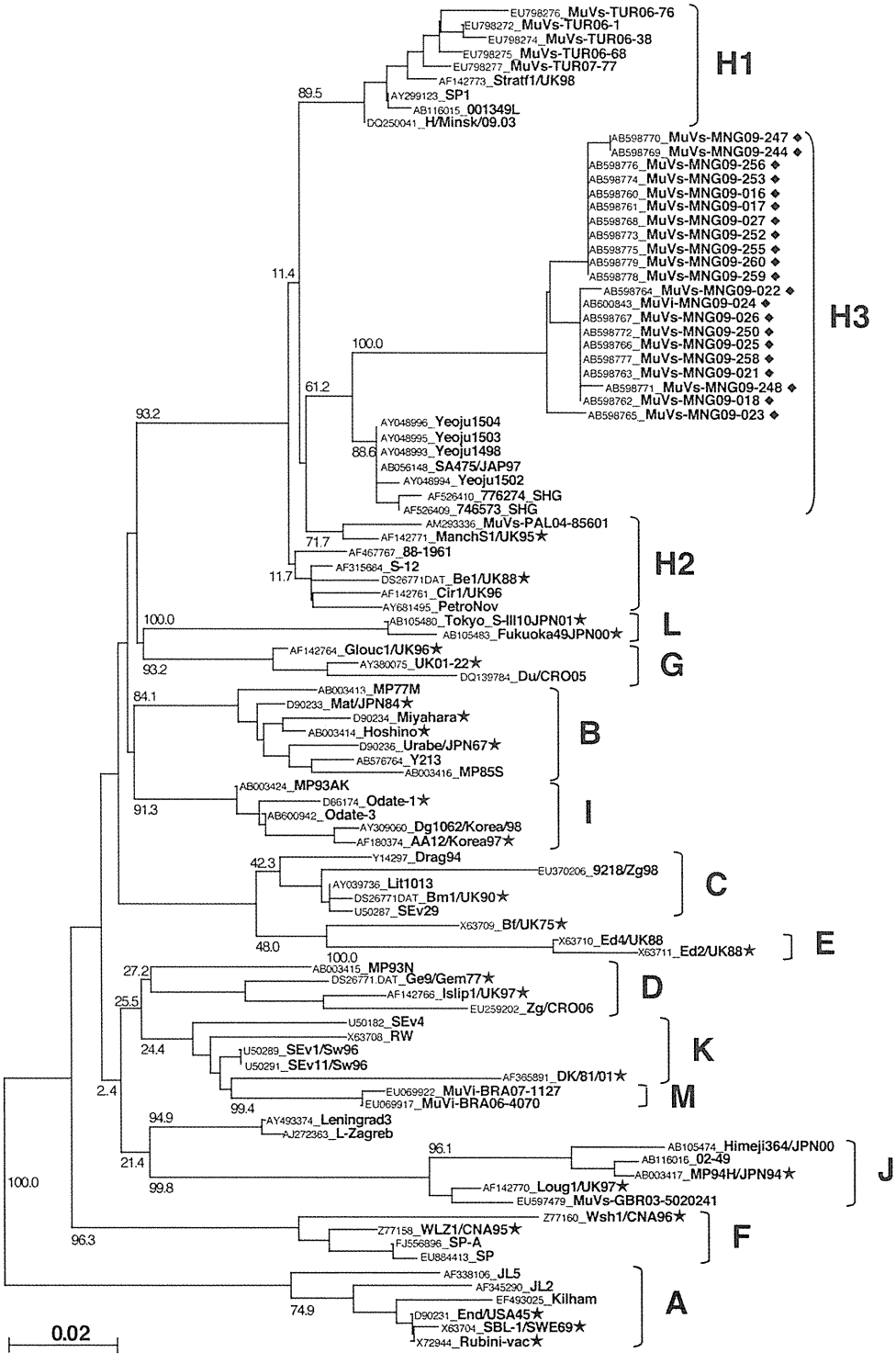

FIG. 2. Phylogenetic relationship between mumps virus strains obtained in the present study and previously published sequences based on the entire SH gene. Genotype A sequences were used as the outgroup. The bar scale indicates the nucleotide substitutions per site. ◆, Mumps virus strains obtained in the present study; ★, reference strains proposed by Jin et al. (15, 41).

the reliability of a phylogenetic relatedness. For instance, the bootstrap value of the SH gene-based lineage group that includes the Mongolian sequences SA475/JPN97, Yeoju1498, Yeoju1502, Yeoju1503, Yeoju1504, 776273SHG, and 776274SHG is relatively low (61.2%, Fig. 2). Meanwhile, the F gene-based lineage group, including the Mongolian sequence and SA475/JPN97 (Fig. 3), or the HN gene-based lineage group, including the Mongolian sequence, Yeoju1498, and Yeoju1502 (Fig. 4), is isolated from the other members of genotype H with high bootstrap values (98.6 and 100%, respec-

TABLE 2. Alignment of deduced amino acid sequences of SH gene of Mongolian strains and genotype H mumps viruses

Strain[a]	Proposed genotype	Consensus amino acid sequence[b]						
		1	10	20	30	40	50	57
Consensus sequence		MPAIQPPLYLTFLLLILLYLIITLYVWITLTITYKTVVRHAALYQRSYFHWSFDHSL						
SA841/JPN00	G	.....						
H/Minsk.Belarus/10.02	H1	.....H.....F.....AA....T.....F.R.....P.						
SP1	H1	.....H.....F.....S.....AA....T.....F.R.....P.						
001349L	H1	....K...H.....F.....S.....AA....T.....F.R.....P.						
V0012	H1	.....H.....F.....S.....AA....T.....F.R.....						
649171_SHG	H1	.....H.....F.....S.....A.....T.....F.R.....P.						
699589_SHG	H1	.....H.....H....F.....S.....AA....T.....F.R.....P.						
763699_SHG	H1	.....H.....F.....S.V...AA....T.....F.R.....P.						
MuVs-TUR06-38H	H1	...V....H.....F.....S.....AA..Y.T.....F.R.....P.						
MuVs-TUR06-76-H	H1	.....H.....M.F.....S.....AA....T.....C.R.....P.						
MuVs-TUR07-77-H	H1	.....H.....F.I...S.....AA....T.....F.R.....P.						
Be1/UK88*	H2	.....N.A....T.....F.R.....P.						
Manch1*	H2	.....H.....A....T.....F.R.....P.						
S-12	H2	.....H.....A....T.....F.R.....P.						
PetroNov	H2	.....S..H.....A....T.....F.R.....P.						
MuVs-PAL04-85601	H2	.....H.....A....T.....L.R.....P.						
88-1961	H2	.....H.....A....T.....F.R.....Q.						
Cir1/UK96	H2	.....H.....N...A....T.....F.R.....P.						
SA475/JPN97	H3	.....H.....C.....I.....A....T.....F.R.....P.						
Yeoju1498	H3	.....H.....C.....I.....A....T.....F.R.....P.						
Yeoju1502	H3	.....H.....C.....I.....A....T.....F.R.....P.						
Yeoju1503	H3	.....H.....C.....I.....A....T.....F.R.....P.						
746573_SHG	H3	.....H.....C.....I.....A....T.....F.R.....P.						
776274_SHG	H3	.....H.....C.....I.....A....T.....F.R...Y.P.						
MuVs-MNG09-023	H3	.....H.....C.....I.....A....T.....FL.....P.						
MuVi-MNG09-024	H3	.....H.....C.....I.....A....T.....FL.....RP.						
MuVs-MNG09-244	H3	.....H.....C.....I.....A...TT.....FL.....RP.						
MuVs-MNG09-248	H3	.....H....S....C.....I.....A....T.....FL.....RP.						

[a] *, Reference strain of genotype H.

[b] The sequences representing each subgenotype strains are listed in this table. In order to highlight the type-specific differences in genotype H sequences, a genotype G sequence (SA841/JPN00 strain, AB056141) was adopted as a consensus amino acid sequence. The numbers above the consensus amino acid sequence show the amino acid residue numbers. Dots in each alignment exhibit amino acids identical to those to the consensus sequence.

tively). These results strongly suggest that Mongolian MuVs may be classified into genotype H and into an individual subgenotype, along with SA475/JPN97, Yeoju1498, Yeoju1502, Yeoju1503, Yeoju1504, and probably 776273SHG and 776274SHG. We propose to name this novel lineage subgenotype H3. The subclassification is also supported by the amino acid sequences of SH genes (Table 2) because all members of this cluster share a specific amino acid pattern at positions 19 and 26 in the SH gene.

Neurovirulence of Mongolian isolate. Several epidemiological studies reported that some genotypes (C, D, H, I, or J) were able to cause central nervous system (CNS) diseases (20, 28, 34–36, 38). Mongolian MuVs belong to genotype H, and all originated from the hospitalized mumps patients. Meanwhile, reliable animal models using common marmosets or neonatal rats to evaluate the neurovirulence of MuV have been proposed (24–27). Therefore, we assessed the neurovirulence of the Mongolian isolate, MuVi-MNG09-024, in a rat model (Fig. 6). As control viruses, we used the Odate-3 (genotype I) and 02-49 (genotype J) strains. Odate-3 is a variant of Odate-1 that caused meningitis with quite high incidence (>70%) in Akita Prefecture, Japan, in 1993 and was isolated during the same period in the same area (28). Odate-3 causes prominent meningitis in common marmosets by peripheral infection (27). The 02-49 strain was isolated in 2001 from the throat swab of a mumps patient with unilateral parotitis in Niigata Prefecture, Japan, and causes moderate hydrocephalus in rats. As expected, Odate-3 caused the most severe hydrocephalus in rats and exhibited the highest NVT score (43.2%) among the three strains. In contrast, the 02-49 strain showed the mildest hydrocephalus (NVT score, 5.6%). MuVi-MNG09-024 shows a moderate result (NVT score, 9.1%). Although the NVT score of MuVi-MNG09-024 is higher than that of 02-49, its scores are below 10%, and there is no significant difference between them ($P = 0.476$). Meanwhile, the NVT score of Odate-3 is significantly different from that of 02-49 and the Mongolian isolate ($P = 0.00004$ and 0.00027, respectively). These results suggest that the Mongolian isolate does not necessarily have highly neurovirulent properties.

DISCUSSION

This is the first report describing the mumps epidemic situation and molecular epidemiological analyses of the circulating MuVs in Mongolia. Interestingly, teenagers comprised the majority of mumps patients by age group during the period of study, and the age distribution of mumps onset is much older than that in Japan, where the <9-year population accounts for more than 90% of all mumps patients. In addition, the ratios of mumps patients in the >20-year age groups have also been consistently increasing over the period. One possible reason for mumps epidemics among the older age groups is due to low

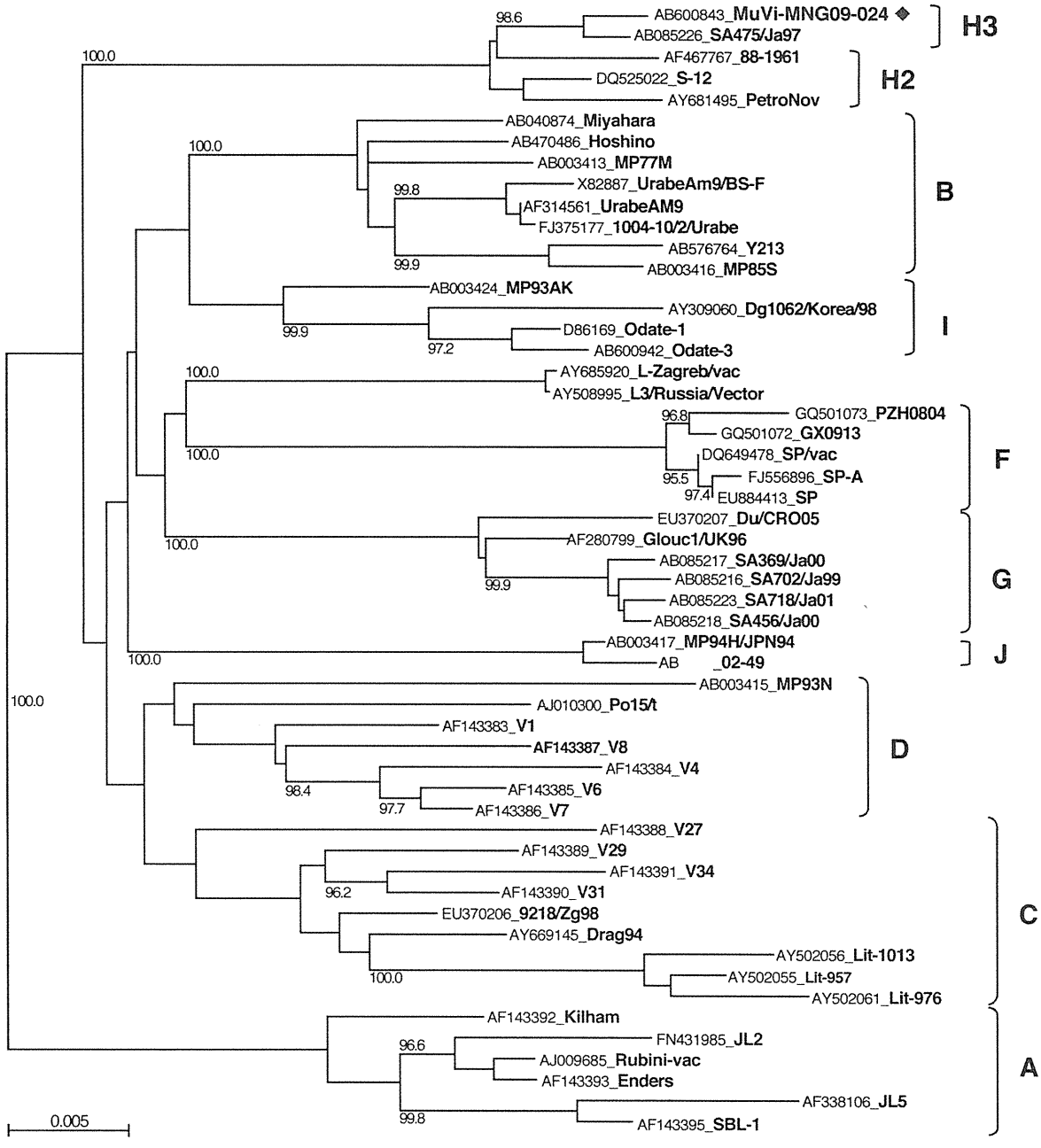

FIG. 3. Phylogenetic tree based on F gene sequences. ◆, Mumps virus strains obtained in the present study.

probabilities of exposure to MuV because of the low population density in Mongolia (two persons per square kilometer). This situation may resemble rural areas of the prevaccine period in the United States (7).

We detected 21 MuV cDNAs from 32 throat swabs of mumps patients in Mongolia. Although the positive ratio of RT-PCR was reasonable (21 of 32), the virus isolation rate was unexpectedly low (1 of 32). The reason for this low frequency of isolation is probably due to freeze-thawing of specimens resulting from insufficient cooling during 5-day transportation from Mongolia to Japan.

By phylogenetic analyses, the SH gene sequences (316 nt) obtained from these Mongolia mumps clinical specimens formed a single cluster, which consists of seven different sequences, and their genetic divergences are >6% (6.3 to 8.2%) compared to the reference strains of the most closely related genotype H. According to the criteria proposed by Jin et al. and the WHO (15, 41), it is plausible that these sequences should be classified into a new genotype based on these results. However, the results of analyses based on F or HN genes or whole-genome sequence data show that the divergences between the Mongolian isolate and other genotype H strains never exceed the within-genotype divergences of other genotypes. Therefore, we concluded that the Mongolian MuVs should be classified into genotype H. Because of its high divergence, the SH gene has been adopted for MuV genotyping.